

Volume 9 | Number 1 | January-December 2020

JCB

Journal of
Circulating Biomarkers



ABOUTSCIENCE

Aims and Scope

Journal of Circulating Biomarkers is an international, peer-reviewed, open access, scientific, online only journal, published once a year. It focuses on all aspects of the rapidly growing field of circulating blood-based biomarkers and diagnostics using circulating protein and lipid markers, circulating tumor cells (CTC), circulating cell-free DNA (cfDNA) and extracellular vesicles, including exosomes, microvesicles, microparticles, ectosomes and apoptotic bodies. The journal publishes high-impact articles that deal with all fields related to circulating biomarkers and diagnostics, ranging from basic science to translational and clinical applications. Papers from a wide variety of disciplines are welcome; interdisciplinary studies are especially suitable for this journal.

Included within the scope are a broad array of specialties including (but not limited to) cancer, immunology, neurology, metabolic diseases, cardiovascular medicine, regenerative medicine, nosology, physiology, pathology, technological applications in diagnostics, therapeutics, vaccine, drug delivery, regenerative medicine, drug development and clinical trials. The journal also hosts reviews, perspectives and news on specific topics.

Indexing

PubMed Central (PMC)

Scopus

DOAJ | Directory of Open Access Journals

CrossRef

OCLC WorldCat

ROAD | Directory of Open Access Scholarly Resources

Opac-ACNP | Catalogo Italiano dei periodici

Opac-SBN | Catalogo del servizio bibliotecario nazionale

Publication process

Peer review

Papers submitted to JCB are subject to a rigorous peer review process, to ensure that the research published is valuable for its readership. JCB applies a single-blind review process and does not disclose the identity of its reviewers.

Lead times

Submission to final decision: 6-8 weeks

Acceptance to publication: 2 weeks

Publication fees

All manuscripts are submitted under Open Access terms. Article processing fees cover any other costs, that is no fee will be applied for supplementary material or for colour illustrations. Where applicable, article processing fees are subject to VAT.

Open access and copyright

All articles are published and licensed under Creative Commons Attribution-NonCommercial 4.0 International license (CC BY-NC 4.0).

Author information and manuscript submission

For full author guidelines and online submission visit

www.aboutscience.eu

EDITORIAL BOARD**Editor in Chief**

Winston Kuo

Predicine Holdings Ltd - Hayward, USA

Associate Editors

Hang Yin - *University of Colorado Boulder, Boulder, USA*

Roger Chammas - *Universidade de Sao Paulo, Sao Paulo, Brazil*

Alain Charest - *Harvard University, Boston, USA*

Clark Chen - *UC San Diego Medical Center, San Diego, USA*

Stefano Fais - *Istituto Superiore di Sanità (National Institute of Health), Rome, Italy*

Ionita Ghiran - *Beth Israel Deaconess Medical Center, Boston, USA*

Nancy Raab-Traub - *University of North Carolina, Chapel Hill, USA*

Lawrence Rajendran - *University of Zurich, Zurich, Switzerland*

John Sinden - *ReNeuron, Bridgend, UK*

Johan Skog - *Exosome Diagnostics, Cambridge, USA*

Alexander Vlassov - *Thermo Fisher Scientific, Austin, USA*

David T. Wong - *University of California Los Angeles, Los Angeles, USA*

Editorial Board

Angel Ayuso-Sacido - *Madrid, Spain*

Leonora Balaj - *Charlestown, USA*

Pauline Carnell-Morris - *Amesbury, UK*

Cesar Castro - *Boston, USA*

Chih Chen - *Hsinchu, China*

Pui-Wah Choi - *Hong Kong*

Emanuele Cocucci - *Columbus, USA*

Utkan Demirci - *Standford, USA*

Dolores Di Vizio - *Los Angeles, USA*

Jiang He - *Charlottesville, USA*

Stefano Holdenrieder - *Munich, Germany*

Bo Huang - *Huazhong, China*

Takanori Ichiki - *Tokyo, Japan*

Alexander Ivanov - *Boston, USA*

Won Jong Rhee - *Incheon, South Korea*

Mehmet Kesimer - *Chapel Hill, USA*

Miroslaw Kornek - *Homburg, Germany*

Masahiko Kuroda - *Tokyo, Japan*

Heedoo Lee - *Changwon, South Korea*

Marcis Leja - *Riga, Latvia*

Sai-Kiang Lim - *Singapore, Singapore*

Aija Line - *Riga, Latvia*

Jan Lotvall - *Gothenburg, Sweden*

Todd Lowe - *Santa Cruz, USA*

Pierre-Yves Mantel - *Fribourg, Switzerland*

David G. Meckes - *Tallahassee, USA*

Andreas Moller - *Brisbane, Australia*

Fatemeh Momen-Heravi - *New York, USA*

Shannon Pendergrast - *Cambridge, USA*

Eva Rohde - *Salzburg, Austria*

Shivani Sharma - *Los Angeles, USA*

Kiyotaka Shiba - *Tokyo, Japan*

Yoshinobu Takakura - *Kyoto, Japan*

Yaoliang Tang - *Georgia, USA*

John Tigges - *Boston, USA*

Matt Trau - *Queensland, Australia*

Jody Vykoukal - *Houston, USA*

ShuQi Wang - *Hangzhou, China*

Gareth Willis - *Boston, USA*

Cynthia Yamamoto - *Irvine, USA*

Milis Yuana - *Utrecht, USA*

Huang-ge Zhang - *Louisville, USA*

Davide Zocco - *Siena, Italy*

ABOUTSCIENCE

Aboutscience Srl

Piazza Duca d'Aosta, 12 - 20124 Milano (Italy)

Disclaimer

The statements, opinions and data contained in this publication are solely those of the individual authors and contributors and do not reflect the opinion of the Editors or the Publisher. The Editors and the Publisher disclaim responsibility for any injury to persons or property resulting from any ideas or products referred to in the articles or advertisements. The use of registered names and trademarks in this publication does not imply, even in the absence of a specific statement, that such names are exempt from the relevant protective laws and regulations and therefore free for general use.

Editorial and production enquiries

jcb@aboutscience.eu

Supplements, reprints and commercial enquiries

Lucia Steele - email: lucia.steele@aboutscience.eu

Publication data

eISSN: 1849-4544

Continuous publication

Vol. 9 (January-December 2020) was published on December 28, 2020

- 1** Exploring adipogenic and myogenic circulatory biomarkers of recurrent pressure injury risk for persons with spinal cord injury
Kath M Bogie, Katelyn Schwartz, Youjin Li, Shengxuan Wang, Wei Dai, Jiayang Sun

- 8** Lung ultrasound and biomarkers in primary care: Partners for a better management of patients with heart failure?
Mar Domingo, Laura Conangla, Josep Lupon, Asunción Wilke, Gladys Juncà, Elena Revuelta-López, Xavier Tejedor, Antoni Bayes-Genis

- 13** Development of an immunofluorescent AR-V7 circulating tumor cell assay – A blood-based test for men with metastatic prostate cancer
David Lu, Rachel Krupa, Melissa Harvey, Ryon P. Graf, Nicole Schreiber, Ethan Barnette, Emily Carbone, Adam Jendrisak, Audrey Gill, Sarah Orr, Howard I Scher, Joseph Daniel Schonhoft

Exploring adipogenic and myogenic circulatory biomarkers of recurrent pressure injury risk for persons with spinal cord injury

Kath M. Bogie^{1,2}, Katelyn Schwartz², Youjin Li³, Shengxuan Wang³, Wei Dai³, Jiayang Sun⁴

¹Case Western Reserve University, Departments of Orthopaedics and Biomedical Engineering, Cleveland, Ohio - USA

²Louis Stokes Cleveland Veterans Affairs Medical Center (LSCVAMC), Research Service, Cleveland, Ohio - USA

³Case Western Reserve University, Department of Population & Quantitative Health Sciences, Cleveland, Ohio - USA

⁴Department of Statistics, George Mason University, Fairfax, Virginia - USA

ABSTRACT

Purpose: To investigate linkages between circulatory adipogenic and myogenic biomarkers, gluteal intramuscular adipose tissue (IMAT), and pressure injury (PrI) history following spinal cord injury (SCI).

Methods: This is an observational repeated-measures study of 30 individuals with SCI. Whole blood was collected regularly over 2-3 years. Circulatory adipogenic and myogenic gene expression was determined. IMAT was defined as above/below 15% (IMATd) or percentage (IMAT%). PrI history was defined as recurrent PrI (RPrI) or PrI number (*n*PrI). Model development used R packages (version 3.5.1). Univariate analysis screened for discriminating genes for downstream multivariate and combined models of averaged and longitudinal data for binary (RPrI/IMATd) and finer scales (*n*PrI/IMAT%).

Results: For adipogenesis, Krüppel-like factor 4 was the top RPrI predictor together with resistin and cyclin D1, and sirtuin 2 was the top IMAT predictor. For myogenesis, the top RPrI predictor was dysferlin 2B, and pyruvate dehydrogenase kinase-4 was the top IMAT predictor together with dystrophin.

Conclusion: Circulatory adipogenic and myogenic biomarkers have statistically significant relationships with PrI history and IMAT for persons with SCI. Biomarkers of interest may act synergistically or additively. Variable importance rankings can reveal nonlinear correlations among the predictors. Biomarkers of interest may act synergistically or additively, thus multiple genes may need to be included for prediction with finer distinction.

Keywords: Adipogenesis genes, Circulatory biomarkers, Myogenesis genes, Recurrent pressure injury, Spinal cord injury

Introduction

Pressure injuries (PrIs) are defined as localized damage to skin and underlying soft tissue that develops due to intense and/or prolonged pressure or pressure combined with shearing (1). PrI can present as intact skin or as open ulcers and can take months or years to heal once developed. Development and/or recurrence of a PrI limits activities of daily living, often leading to hospitalization and even death. Padula

et al (2) reported that from 2011 to 2014 there were 60,000 reported deaths due to PrI. PrI management is also expensive: Management of hospital-acquired PrI (HAPI) alone has been reported to cost US healthcare over \$26 billion annually (3). Management costs for community-acquired PrI have yet to be determined but may be presumed to be at least \$8 billion (30% of HAPI costs).

Spinal cord injury (SCI) is defined as damage to any part of the spinal cord or nerves at the end of the spinal canal. Traumatic SCI occurs suddenly due to a blow or cut to the spine, such as can occur in a motor vehicle accident or fall. SCI often leads to permanent loss of strength, sensation, and function below the site of the injury. A complete SCI will result in total loss of all motor and sensory function below the level of injury, while with an incomplete SCI there can be some sensory and/or motor function retained. During the acute and subacute stages following injury, there can be some neurorecovery. Once neurorecovery has plateaued, the condition is considered to be chronic SCI (4). This is most commonly considered to be 1 year following traumatic injury.

Received: April 9, 2020

Accepted: August 18, 2020

Published online: September 21, 2020

Corresponding author:

Kath M. Bogie
Louis Stokes Cleveland Veterans Affairs Medical Center
10701 East Blvd
Cleveland, OH 44106 - USA
kmb3@case.edu

Persons with SCI remain at risk for PrI development throughout their lifetime and often develop community-acquired PrI. PrI remain one of the most devastating secondary complications for persons living with SCI. It remains unclear why some persons with SCI suffer from a continuous cycle of recurring PrI, while others remain PrI free.

The National Pressure Injury Advisory Panel has recognized that some PrI might be unavoidable due to complex and systemic intrinsic factors (5). In response to these intrinsic factors, biomarkers that signal tissue health status are released into circulation. Circulatory messenger ribonucleic acid (mRNA) biomarkers related to fatty metabolism, which are valuable risk indicators for PrI risk, have previously been reported (6). Factors that regulate and control downstream biomarker production related to fatty metabolism, specifically adipogenesis and myogenesis, are thus of interest for determining the risk of developing recurrent PrI (RPrI).

The study objective was to evaluate relationships between circulatory adipogenic and myogenic biomarkers, PrI history, and muscle composition, in persons with chronic SCI, by secondary analysis of preexisting blood samples.

Methods

A repeated-measures study design was employed. Individuals with complete or incomplete SCI were recruited: Exclusion criteria included having an open pelvic region PrI and presence of a systemic disease. A comprehensive demographic profile was obtained at enrolment. Whole blood samples were obtained every 6 to 12 months over 2-3 years. The study was carried out at a tertiary care facility. All clinical study activities were reviewed and approved by the local

Institutional Review Board and by the US Army Human Research Protection Office.

Blood sample collection

Whole blood samples were collected for quantitative reverse transcription polymerase chain reaction (RT-qPCR) analysis. Samples were frozen immediately in a -80°C freezer prior to further processing. Samples from participants who met the eligibility criteria of either having no PrI history or having a history of RPrI were selected for secondary analysis focused on circulatory adipogenic and myogenic biomarkers (Fig. 1).

RT-qPCR analysis

RNA was extracted from whole blood samples using QIAzol Lysis reagent and the Qiagen Mini Kit (Qiagen, Valencia, CA) following the RNA extraction protocol provided in each kit. Immediately following completion of RNA isolation, sample concentration was measured using the NanoDrop ND-2000. Sample yields between 25 and 200 ng/ μL of RNA and A260:A280 ratios between 1.8 and 2.0 were used for further processing. RNA Integrity Number (RIN) was determined using fluorometric quantification (Qubit, Fisher Scientific Singapore) and confirmed using the Agilent Bioanalyzer. Verification of 18S and 28S ribosomal RNA integrity was analyzed by agarose gel electrophoresis and Agilent Bioanalyzer electropherograms.

The thermocycler was used for complementary deoxyribonucleic acid (cDNA) synthesis; 200 ng RNA from each sample was mixed with Buffer GE and nuclease-free water from

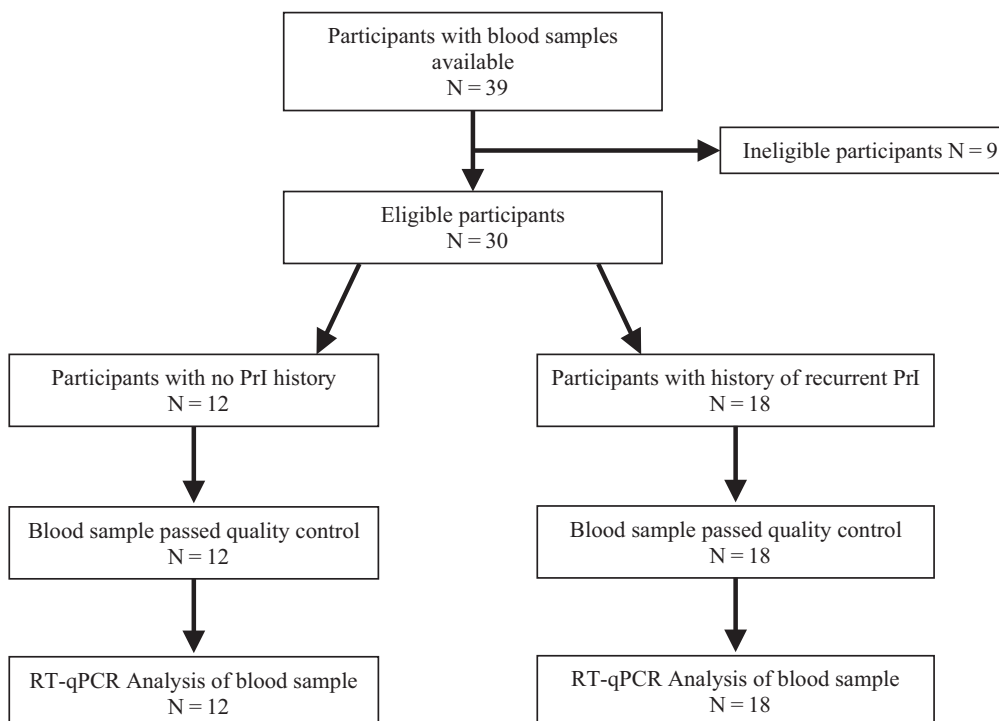


Fig. 1 - Observational study: flow chart for secondary analysis of blood samples for model development

the Qiagen RT² First Strand kit (Qiagen, Valencia, CA). At stage 2, the RT mix (Qiagen, RT² First Strand Kit, Valencia, CA) was added to the RNA solution and the sample was left to run for the remaining stages. Nuclease-free water (Qiagen, RT² First Strand Kit, Valencia, CA) was added after cDNA synthesis was completed. The cDNA was mixed with nuclease-free water (Qiagen, Valencia, CA) and SYBR Green ROX qPCR Master Mix (Qiagen, Valencia, CA) based on the Qiagen RT² Profiler PCR array handbook. Commercially available custom RT² Profiler PCR array plates (PAHS-049ZA and PAHS-099ZA) were employed to determine expression of over 100 genes involved in adipogenesis and myogenesis.

RT-qPCR analysis was run using a 96-fast plate SYBR Green qPCR protocol on an ABI ViiA7 platform (Applied Biosystems, Foster City, CA, USA) by the standard curve method. Each well contained 25 μ L total reaction volume. The protocol included 1 cycle for 10 minutes at 95°C to activate the HotStart DNA Taq Polymerase followed by 40 cycles of 2-step RT-qPCR, including 15 seconds at 95°C and 1 minute at 60°C where fluorescence data collection was performed. Ramp rates were adjusted to 1°C/s. Lastly, a 1-cycle melting curve verified RT-qPCR specificity according to the RT² Profiler PCR array handbook.

Raw Ct (cycle threshold) values were loaded into qbase+ software (BioGazelle, Zwijnaarde, Belgium) to compute Calibrated Normalized Relative Quantities (CNRQ) for further data analysis. Inhibition testing used RT control and positive PCR control wells on the custom array plates. Ct values across all PCR array runs were analyzed for sufficient quality by the value of the C_T^{PPC} wells of 20 ± 2 . Values outside this threshold were eliminated from analysis. General DNA contamination was observed by analyzing the raw Ct values of the human genomic DNA contamination (HGDC) well on each plate and eliminating sample runs with values less than 35 Ct in the HGDC well. A control Ct value less than 35 indicated the presence of detectable genomic DNA contamination as recommended by the Qiagen RT² Profiler PCR array handbook.

Reference genes (beta-2-microglobulin, actin, hypoxanthine phosphoribosyltransferase-1, and large ribosomal protein P0) were included in custom plate arrays from Qiagen. Normalization methods were automated through qbase+ software.

Gluteal intramuscular adipose tissue (IMAT) content was determined following a previously developed standardized protocol (7).

Demographics

Repeated evaluations were completed for 30 participants with complete or incomplete SCI. Study participants had either a history of multiple PrI (Group I) or no history of PrI (Group II). Study groups were comparable with respect to standard demographic measures as shown in Table I.

Statistical methods

As with most studies using multivariate PCR arrays, not all genes were present for all samples. Merely deleting any gene (the column variable) or any observation (the row

TABLE I - Study participant demographics

| | | Group I PrI | | Group II No PrI | |
|---------------------------|--------------------------|----------------|-----|--------------------|-----|
| N | 29 | 18 | | 12 | |
| Age at injury | Range | 22-75 | | 22-71 | |
| | Mean | 46.3 | | 50.2 | |
| Age at study | Range | 33-81 | | 30-74 | |
| | Mean | 57.5 | | 57.6 | |
| Sex | Male | 16 | 89% | 11 | 92% |
| | Female | 2 | 11% | 1 | 8% |
| Duration of injury | Range | 9 mo-46 y | | 1 mo-34 y | |
| | Mean | 13.8 y | | 7.5 y | |
| Neurological level | Above T6 | 12 | 67% | 9 | 75% |
| | Below T6 | 6 | 33% | 3 | 25% |
| ASIA Level | Complete (AIS = A) | 7 | 39% | 2 | 17% |
| | Incomplete (AIS = B,C,D) | 11 | 61% | 10 | 83% |

AIS = American Spinal Injury Association Impairment Scale; PrI = pressure injury.

variable) with *any* missing values would both eliminate too many observations and lead to a biased sample, since there is a low detection limit (LDL) for each gene. In the current study, genes with more than 70% missing were excluded from all analysis. To overcome the LDL issue, missing values for the remaining genes were imputed before a downstream analysis and the missing information directly incorporated in the next stage analysis. The imputed values were determined to be an estimated conditional mean of gene expression, given that the expression is known to be smaller than the detection limit defined by qbase+, or a scaled minimum observed value, as suggested by Nie et al (8). The minimum observed values of normalized expressions were negative if gene activity was less than the normalization factors. We examined the effect of imputation by the conditional mean, and 1, $\sqrt{2}$, and 2 times the minimum observed. It was found that each approach gave similar results. Hence, the results using $\sqrt{2}$ as the scaling factor are presented.

Comprehensive analyses were carried out on data with longitudinal repeated measures and on data averaged over time to find the factors that influence PrI outcomes. Meaningful outcomes were defined as the number of PrI ($nPrI$) and the percent of IMAT (IMAT%) since IMAT has been found to be a major risk factor for PrI in earlier analysis (7,9). The dichotomized versions of these two outcomes were “with or without pressure injury” (RPrI) and “below or above 15% IMAT” (IMATd).

Data analyses were performed using statistical software program R (version 3.5.1) with packages *rpart* (for tree-based modeling), *lme4* (for linear mixed effects modeling), *gee-pack* (for Generalized Estimating Equation [GEE] modeling), *glmnet* (for least absolute shrinkage and selection operator [LASSO] on generalized linear models), and *glmLasso* (for

LASSO on generalized linear mixed models). Due to the large number of genes relative to the number of subjects (large *p* problem), our comprehensive analyses included univariate, multivariate, and combined analyses.

Univariate analyses

Each gene was examined to see if it was discriminated between the dichotomized outcomes of interest, specifically RPrI and IMATd. The statistical methods for group comparisons are given below:

Group comparison via confidence interval on data averaged over time

For each gene, the *t*- and bootstrap confidence intervals (CIs) of each group mean were used to check the CI overlap for contrasting groups. The absence of any overlap approximated a significant group mean difference at 0.05, based on the CI levels recommended by Payton et al (10).

Group comparison via survival models

Gene expression data can be considered as left-censored data, that is, values below the detection limit are censored. Thus, survival models were applied treating data without missing values as an event and data with missing values as censored. In this case, "longer survival time" is equivalent to higher gene expression values. Both a parametric procedure based on the log-normal distribution and the Kaplan–Meier, a nonparametric survival analysis procedure, were used to check group differences based on RPrI and IMATd for each gene.

Variable importance rankings from the parametric model are presented for important adipogenesis (Tab. II) and myogenesis genes (Tab. III). Genes selected by this prescreening procedure were then included for downstream analyses using multivariate and combined approaches.

Multivariate analyses

Tree-based models and penalized regression procedures using LASSO are suitable for finding important factors for large-*p* data. For averaged data over time, tree-based models on dichotomized RPrI and IMATd including all eligible genes were first performed. Tree-based models handle missing values by using surrogates. The variable importance ranking from these models is indicative of the candidate genes for the final modeling.

LASSO performs variable selection and prediction from a complex dataset simultaneously. Two LASSO R packages were used: *glmnet* for averaged data and *glmLasso* for longitudinal data with a random intercept. Variables of interest were also analyzed on the finer scale. Poisson regression was applied to *nPrI*. Gaussian regression was applied to the logit transformed IMAT%.

For averaged data, the penalization level was set by both fivefold cross-validation (CV) and minimizing the Bayesian information criterion (BIC). For longitudinal data the

TABLE II - Binary outcomes: variable importance ranking for adipogenesis genes

| Gene name | Standard abbreviation | Ranking |
|--|-----------------------|---------|
| (a) RPrI as outcome | | |
| | IMAT% | 6.01 |
| Kruppel-like factor 4 | KLF4 | 3.21 |
| Retinoblastoma 1 | RB1 | 2.25 |
| Cyclin-dependent kinase inhibitor 1A | CDKN1A | 1.50 |
| Fatty acid synthase | FASN | 1.50 |
| Insulin receptor substrate 2 | IRS2 | 1.50 |
| Lamin A/C | LMNA | 1.50 |
| (b) IMATd as outcome | | |
| Sirtuin 2 | SIRT2 | 4.80 |
| Complement factor D (adipsin) | CFD | 2.40 |
| Cyclin-dependent kinase inhibitor 1B | CDKN1B | 1.92 |
| Insulin receptor substrate 2 | IRS2 | 1.92 |
| Sterol regulatory element binding transcription factor 1 | SREBF1 | 1.92 |
| Tafazzin | TAZ | 1.92 |

IMATd = below or above 15% intramuscular adipose tissue; RPrI = recurrent pressure injury.

TABLE III - Binary outcomes: variable importance ranking for myogenic genes

| Gene name | Standard abbreviation | Ranking |
|--|-----------------------|---------|
| (a) RPrI as outcome | | |
| | IMAT% | 6.01 |
| Dysferlin 2B | DYSF2B | 2.76 |
| Mitogen-activated protein kinase 1 | MAPK1 | 2.76 |
| Lamin A/C | LMNA | 2.25 |
| Calpain 3 | CAPN3 | 1.88 |
| AKT serine/threonine kinase 1 | AKT1 | 1.50 |
| Mitogen-activated protein kinase 14 | MAPK 14 | 1.50 |
| Caspase 3, apoptosis related | CASP3AR | 1.26 |
| Adrenoceptor beta 2 | ADRB2 | 1.26 |
| Myocyte enhancer factor 2C | MEF2C | 1.26 |
| (b) IMATd as outcome | | |
| Pyruvate dehydrogenase kinase 4 | PDK4 | 5.09 |
| Lamin A/C | LMNA | 2.78 |
| Matrix metalloproteinase 9 | MMP9 | 2.78 |
| Transforming growth factor beta 1 | TGFB1 | 2.78 |
| Ribosomal protein S6 kinase, polypeptide 1 | RPS6KA1 | 2.31 |
| Utrophin | UTRN | 2.31 |

IMATd = below or above 15% intramuscular adipose tissue; RPrI = recurrent pressure injury.

penalization level was set only by minimizing BIC due to high computational cost in using CV.

GEEs using the selected genes from longitudinal LASSO were also fit to serve as a complementary “sanity check” for the effects of the selected genes. As above, a possibly significant effect was defined as having a $p < 0.05$. A marginal effect was defined as having a $p > 0.05$ but < 0.10 .

Regression combining the results from univariate and multivariate analyses

Genes found to be important from either the univariate analyses or one of the multivariate analyses were selected into a preliminary candidate set. A further combined analysis was then conducted using generalized linear mixed models to evaluate the feasibility of a more parsimonious model. Three candidate analysis procedures/models were applied (Tree, GLMM LASSO, and combined GLMM) using both binary (RPri/IMATd) and finer scales (n Pri/IMAT%) on averaged data and longitudinal data with a random intercept. All the reported Poisson GLMM models passed the “over-dispersion” test.

Results

Following SCI, there is a loss of muscle mass and changes in muscle fiber type (11), which has some similarities to sarcopenia. Acutely following injury, there is a rapid and dramatic loss of muscle mass over a period of weeks or months. It has also been shown that composition of the paralyzed muscle also changes (9): dystrophic-type changes occur in muscles with the lean muscle tissue replaced by adipose tissue, that is, fatty infiltration, or IMAT, increases. These changes in composition continue, even several years following injury. IMAT has been reported to increase with aging in healthy adults (12), with an increase of around 3% annually for persons over 50 years (13). However, following SCI, the rapid IMAT accumulation seen in some individuals is occurring both more quickly and at a younger age than would be expected for sarcopenic muscle changes (9). Higher IMAT compromises tissue resilience by reducing the overall microvasculature of the affected composite muscle tissue. The remaining blood vessels are also more prone to occlude under load. These changes thus impair the response to applied loads and increase the risk of tissue breakdown and Pri development. Changes in adiposity do not appear to be associated or correlated with clinical or demographic factors such as level or extent of injury (9,14). It is also important to clarify that in the same way as cholesterol levels vary independent of body mass index (BMI), so higher levels of IMAT deposition are not correlated with SCI-adjusted BMI.

There is growing appreciation that there is increased sub-clinical inflammatory activity following SCI (15-17), which has recently been confirmed by functional genomics (18). When inflammation is prolonged by dysregulation, it can have harmful effects on tissue. However, prior work has shown that while inflammatory biomarkers can be detected in the circulation of persons with SCI, they are not discriminatory for RPri risk (6). The role of fatty infiltration, or intramuscular adipose tissue, has only recently been reported (7,9).

Relationships between adipogenic and myogenic circulatory biomarkers and RPri in persons living with SCI have not previously been reported.

In the current study, results from different models were relatively consistent for identifying most important genes with a statistically significant effect on Pri history or IMAT. All the genes with a significant p value (< 0.05) for the regression modeling combining univariate and multivariate analyses were considered together with those that have a marginal p value (< 0.10) from most tests.

Adipogenic circulatory biomarkers

Using RPri as the outcome measure, IMAT% is the top variable and Krüppel-like factor (KLF4) the top adipogenesis gene that complements IMAT in predicting Pri (Tab. IIa). KLF4 supports energy demand in skeletal muscle (19) and has been suggested as a potentially significant inhibitor of adipose biology (20). When IMATd was defined as the primary model outcome, the adipogenesis tree model indicated sirtuin 2 (SIRT2) was the critical determinant (Tab. IIb). The importance of SIRT2 as an adipogenesis gene for IMAT is also shown by both GLMM with a LASSO penalty and the combined GLMM analysis (Tab. V). SIRT2 inhibits lipid synthesis, playing a role in glyceroneogenesis or fat deposition into adipose tissue (21). Thus, increased SIRT2 expression may play a role in IMAT deposition over time following SCI.

In the combined GLMM analysis for n Pri, a finer scale than RPri, in addition to IMAT, important adipogenesis genes included GATA binding protein 2 (GATA2), resistin (RETN), and cyclin D1 (CCND1) (Tab. IV).

We also found retinoblastoma 1 (RB1) to be a significant factor in models fit for RPri (Tab. IIa) and in the multivariate adipogenesis model using IMAT% as outcome (Tab. V). RB1 expression is an important factor in adipocyte differentiation (22). It is negatively associated with BMI in able-bodied individuals, but positively associated with adipogenesis regulators such as peroxisome proliferator-activated receptor gamma (PPAR γ). Current results suggest RB1 levels are reduced in environments that limit adipogenesis. Complement factor D (CFD), also known as adipsin, is an important factor in the binary adipogenesis model with IMATd as outcome (Tab. IIb).

TABLE IV - Poisson generalized linear mixed model using n Pri as outcome for adipogenesis (conditional $R^2 = 0.73$)

| Gene name | Standard abbreviation | Estimate | Std. | z value | Pr(> z) |
|------------------------|-----------------------|----------|-------|---------|----------|
| | (Intercept) | 0.359 | 0.346 | 1.04 | 0.2990 |
| | IMAT% | 2.479 | 0.852 | 2.91 | 0.0036 |
| GATA binding protein 2 | GATA2 | 0.355 | 0.890 | 0.4 | 0.6900 |
| Resistin | RETN | 1.116 | 0.694 | 1.61 | 0.1080 |
| Cyclin D1 | CCND1 | 0.582 | 0.246 | 2.36 | 0.0180 |
| | Months | -0.001 | 0.016 | -0.05 | 0.9599 |

IMAT = intramuscular adipose tissue; n Pri = recurrent pressure injury number.

TABLE V - Linear mixed model using logit(IMAT) as outcome for adipogenesis (conditional $R^2 = 0.98$)

| Gene name | Standard abbreviation | Estimate | Std. | t value | Pr(> t) |
|--------------------------------|-----------------------|----------|-------|---------|----------|
| | (Intercept) | -2.252 | 0.408 | -5.53 | 0.00001 |
| Nuclear receptor coactivator 2 | NCOA1 | 2.453 | 1.054 | 2.33 | 0.0518 |
| Resistin | RETN | -0.964 | 0.420 | -2.29 | 0.0631 |
| Sirtuin 2 | SIRT2 | 1.486 | 0.599 | 2.48 | 0.0448 |
| Sirtuin 3 | SIRT3 | -2.621 | 0.584 | -4.49 | 0.0034 |
| retinoblastoma 1 | RB1 | -3.328 | 0.648 | -5.14 | 0.0015 |
| retinoid X receptor, alpha | RXRA | 2.658 | 0.648 | 4.10 | 0.0074 |
| | Months | -0.051 | 0.010 | -5.08 | 0.0017 |

IMAT = intramuscular adipose tissue.

CFD is exclusively expressed in adipose tissue and is a rate-limiting component of the alternative complement pathway that regulates innate immune response (23).

Myogenic circulatory biomarkers

For myogenesis, in addition to PrI, the top gene that works with IMAT is dysferlin 2B (DYSF2B) to predict RPrI (Tab. IIIa) and pyruvate dehydrogenase kinase 4 (PDK4) for predicting IMATd (Tab. IIIb). Although included on a myogenesis panel, PDK4 also contributes to glucose metabolism regulation, facilitating glyceroneogenesis and triacylglycerol storage (24). The current models also showed PDK4 to be a useful but not significant factor in multivariate myogenesis models with IMAT as the outcome (Tab. VII).

The binary myogenesis tree model (Tab. IIIa) indicates that *DYSF2B* expression is a myogenic determinant for RPrI. Lack of *DYSF2B* causes changes in myofiber repair, alters calcium homeostasis, and causes chronic muscle inflammation (25). Muscle loss due to myofiber replacement with fibrotic or adipogenic tissue is well known in chronic muscle injuries, but has not previously been studied in persons with chronic SCI. Muscle damage and regeneration are exacerbated by increased levels of fibro/adipogenic precursors (FAPs), which cause adipogenic replacement of muscle fibers in tissues with mutated dysferlin (25).

GLMM with a LASSO penalty indicated *DYSF2B* as an important gene in the multivariate myogenesis models for *nPrI* (Tab. VI). For the combined GLMM analysis, dystrophin (DMD) also appeared to be more significant in the combined model when logit(IMAT) is the outcome measure (Tab. VII). PDK4 was also included in the final models but with *p* values larger than 0.10 (Tab. VII).

Limitations

This exploratory study involved a moderately sized cohort followed for up to 3 years. Variations between univariate and

TABLE VI - Poisson generalized linear mixed model using *nPrI* as outcome for myogenesis (conditional $R^2 = 0.75$)

| Gene name | Standard abbreviation | Estimate | Std. | z value | Pr(> z) |
|---------------------|-----------------------|----------|-------|---------|----------|
| | (Intercept) | -0.220 | 0.297 | -0.74 | 0.4595 |
| | IMAT% | 2.674 | 0.859 | 3.11 | 0.0019 |
| Dysferlin 2B | DYSF2B | 1.061 | 0.692 | 1.53 | 0.1252 |
| Hexokinase 2 | HK2 | -1.132 | 1.002 | -1.13 | 0.2587 |
| Interleukin 1, beta | IL-1B | 1.138 | 0.806 | 1.41 | 0.1578 |
| | Months | -0.003 | 0.016 | -0.18 | 0.8608 |

IMAT = intramuscular adipose tissue; *nPrI* = recurrent pressure injury number.

TABLE VII - Linear mixed model using logit(IMAT) as outcome for myogenesis (conditional $R^2 = 0.72$)

| Variable name | Standard abbreviation | Estimate | Std. | t value | Pr(> t) |
|---------------------------------|-----------------------|----------|-------|---------|----------|
| | (Intercept) | -2.067 | 0.376 | -5.49 | 0.000003 |
| Matrix metalloproteinase 9 | MMP9 | 0.641 | 0.621 | 1.03 | 0.3100 |
| Pyruvate dehydrogenase kinase 4 | PDK4 | 0.173 | 0.644 | 0.27 | 0.7910 |
| Dystrophin | DMD | 0.401 | 0.194 | 2.07 | 0.0490 |
| | Months | 0.002 | 0.018 | 0.12 | 0.9040 |

IMAT = intramuscular adipose tissue.

multivariate models for adipogenesis indicate some difference in pathways for PrI development and IMAT. For myogenesis, the results across all analyses are more consistent. Further work is needed to clarify the impact on PrI risk over time of genes of interest involved in adipogenesis and myogenesis.

Conclusions

Persons with SCI have a near-normal life expectancy if they do not develop severe secondary complications, in particular PrI. While this is a lifetime risk, it also appears that susceptibility for this devastating secondary complication is unique for each individual. These differences are not clearly associated with either level of injury or American Spinal Injury Association Impairment Scale (AIS) grade. This exploratory analysis confirms that IMAT is a major indicator for RPrI risk. Circulatory adipogenic and myogenic biomarkers have statistically significant relationships with PrI history and IMAT. The models indicated the importance of each gene based on the sum of the improvements in all nodes. Variable importance rankings can reveal nonlinear correlations among the predictors. Biomarkers of interest may act synergistically or additively, thus multiple genes may need to be included for prediction with finer distinction.

Data availability statement

Data cannot be shared publicly due to the policies of our institution. Data may be made available to researchers who meet the criteria for access to confidential data following review by the Institutional Data Access Committee (contact via Dr. KM Bogie).

Disclosures

Conflict of interest: The authors report grants from CDMRP Spinal Cord Injury Research Program and grants from Craig H. Neilsen Foundation during the conduct of the study.

Financial support: The work described in this article was supported by the CDMRP Spinal Cord Injury Research Program (grant no. W81XWH-14-1-0618) and the Craig H. Neilsen Foundation (grant no. 315537).

References

1. Henzel MK, Bogie KM. Medical management of pressure ulcers in patients with spinal cord disorders. In: Kirshblum S, Lin VW, eds. *Spinal cord medicine*, 3rd ed. Springer 2018;516-543.
2. Padula WV, Pronovost PJ, Makic MBF, et al. Value of hospital resources for effective pressure injury prevention: a cost-effectiveness analysis. *BMJ Qual Saf*. 2019 Feb;28(2):132-141.
3. Padula WV, Delarmente BA. The national cost of hospital-acquired pressure injuries in the United States. *Int Wound J*. 2019 Jun;16(3):634-640.
4. Burns AS, Marino RJ, Flanders AE, Flett H. Clinical diagnosis and prognosis following spinal cord injury. *Handb Clin Neurol*. 2012;109:47-62.
5. Edsberg LE, Langemo D, Baharestani MM, Posthauer ME, Goldberg M. Unavoidable pressure injury: state of the science and consensus outcomes. *J Wound Ostomy Continence Nurs*. 2014 Jul-Aug;41(4):313-334.
6. Schwartz K, Henzel MK, Ann Richmond M, et al. Biomarkers for recurrent pressure injury risk in persons with spinal cord injury. *J Spinal Cord Med*. 2019 Sep 6:1-8.
7. Wu GA, Bogie KM. Not just quantity: gluteus maximus muscle characteristics in able-bodied and SCI individuals--implications for tissue viability. *J Tissue Viability*. 2013 Aug;22(3):74-82.
8. Nie L, Chu H, Liu C, Cole SR, Vexler A, Schisterman EF. Linear regression with an independent variable subject to a detection limit. *Epidemiology*. 2010 Jul;21 Suppl 4:S17-S24.
9. Lemmer DP, Alvarado N, Henzel K, et al. What lies beneath: why some pressure injuries may be unpreventable for individuals with spinal cord injury. *Arch Phys Med Rehabil*. 2019 Jun;100(6):1042-1049.
10. Payton ME, Greenstone MH, Schenker N. Overlapping confidence intervals or standard error intervals: what do they mean in terms of statistical significance? *J Insect Sci*. 2003;3:34.
11. Castro MJ, Apple DF Jr, Staron RS, Campos GE, Dudley GA. Influence of complete spinal cord injury on skeletal muscle within 6 mo of injury. *J Appl Physiol*. 1999 Jan;86(1):350-358.
12. Marcus RL, Addison O, Kidde JP, Dibble LE, Lastayo PC. Skeletal muscle fat infiltration: impact of age, inactivity, and exercise. *J Nutr Health Aging*. 2010 May;14(5):362-366.
13. Yoshiko A, Hioki M, Kanehira N, et al. Three-dimensional comparison of intramuscular fat content between young and old adults. *BMC Med Imaging*. 2017 Feb 10;17(1):12.
14. Farkas GJ, Gorgey AS, Dolbow DR, Berg AS, Gater DR. The influence of level of spinal cord injury on adipose tissue and its relationship to inflammatory adipokines and cardiometabolic profiles. *J Spinal Cord Med*. 2018 Jul;41(4):407-415.
15. Wang TD, Wang YH, Huang TS, Su TC, Pan SL, Chen SY. Circulating levels of markers of inflammation and endothelial activation are increased in men with chronic spinal cord injury. *J Formos Med Assoc*. 2007 Nov;106(11):919-928.
16. Morse LR, Stolzmann K, Nguyen HP, et al. Association between mobility mode and C-reactive protein levels in men with chronic spinal cord injury. *Arch Phys Med Rehabil*. 2008 Apr;89(4):726-731.
17. Radulovic M, Bauman WA, Wecht JM, et al. Biomarkers of inflammation in persons with chronic tetraplegia. *J Breath Res*. 2015 May 14;9(3):036001.
18. Herman P, Stein A, Gibbs K, Korsunsky I, Gregersen P, Bloom O. Persons with chronic spinal cord injury have decreased natural killer cell and increased toll-like receptor/inflammatory Gene Expression. *J Neurotrauma*. 2018 Aug 1;35(15):1819-1829.
19. Hsieh PN, Fan L, Sweet DR, Jain MK. The Krüppel-Like factors and control of energy homeostasis. *Endocr Rev*. 2019 Feb 1;40(1):137-152. PMID: 30307551; PMCID: PMC6334632.
20. Eisenstein A, Carroll SH, Johnston-Cox H, Farb M, Gokce N, Ravid K. An adenosine receptor-Krüppel-like factor 4 protein axis inhibits adipogenesis. *J Biol Chem*. 2014 Jul 25;289(30):21071-21081.
21. Gomes P, Fleming Outeiro T, Cavadas C. Emerging role of Sirtuin 2 in the regulation of mammalian metabolism. *Trends Pharmacol Sci*. 2015 Nov;36(11):756-768.
22. Moreno-Navarrete JM, Petrov P, Serrano M, et al. Decreased RB1 mRNA, protein, and activity reflect obesity-induced altered adipogenic capacity in human adipose tissue. *Diabetes*. 2013 Jun;62(6):1923-1931.
23. Li Y, Zou W, Brestoff JR, Rohatgi N, et al. Fat-produced adiponectin regulates inflammatory arthritis. *Cell Rep*. 2019 Jun 4;27(10):2809-2816.e3.
24. Holness MJ, Zariwala G, Walker CG, Sugden MC. Adipocyte pyruvate dehydrogenase kinase 4 expression is associated with augmented PPAR γ upregulation in early-life programming of later obesity. *FEBS Open Bio*. 2012 Mar 5;2:32-36.
25. Hogarth MW, Defour A, Lazarski C, et al. Fibroadipogenic progenitors are responsible for muscle loss in limb girdle muscular dystrophy 2B. *Nat Commun*. 2019 Jun 3;10(1):2430.

Lung ultrasound and biomarkers in primary care: Partners for a better management of patients with heart failure?

Mar Domingo^{1,3}, Laura Conangla^{1,3}, Josep Lupón^{1,4,5}, Asunción Wilke^{2,4}, Gladys Juncà¹, Elena Revuelta-López^{1,5,6}, Xavier Tejedor⁷, Antoni Bayes-Genis^{1,4,5}

¹Heart Failure Unit and Cardiology Department, Hospital Universitari Germans Trias i Pujol, Badalona - Spain

²Primary Care Service Barcelonès Nord i Maresme, Catalan Health Institute, Badalona - Spain

³Institut Universitari d'Investigació en Atenció Primària Jordi Gol (IDIAP Jordi Gol), Barcelona - Spain

⁴Department of Medicine, Universitat Autònoma de Barcelona, Barcelona - Spain

⁵CIBERCV, Instituto de Salud Carlos III, Madrid - Spain

⁶ICREC Research Program, Germans Trias i Pujol Health Science Research Institute, Can Ruti Campus, Badalona - Spain

⁷Biochemistry Service, Hospital Universitari Germans Trias i Pujol, Badalona - Spain

ABSTRACT

Introduction: The association of pulmonary congestion assessed by lung ultrasound (LUS) and biomarkers—other than N-terminal pro-brain natriuretic peptide (NT-proBNP)—is uncertain.

Methods: We investigated the relationship between total B-line count by LUS and several biomarkers in outpatients with suspicion of heart failure (HF). Primary care patients with suspected new-onset nonacute HF were evaluated both with a 12-scan LUS protocol (8 anterolateral areas plus 4 lower posterior thoracic areas) and 11 inflammatory and cardiovascular biomarkers. A cardiologist blinded to LUS and biomarkers except NT-proBNP confirmed HF diagnosis. After log-transformation of biomarkers' concentrations, unadjusted and adjusted correlations were performed.

Results: A total of 170 patients were included (age 76 ± 10 years, 67.6% women). HF diagnosis was confirmed in 38 (22.4%) patients. After adjustment by age, sex, body mass index, and renal function, total B-line sum significantly correlated with NT-proBNP ($R = 0.29$, $p < 0.001$), growth/differentiation factor-15 (GDF-15; $R = 0.23$, $p = 0.003$), high-sensitive Troponin T (hsTnT; $R = 0.36$, $p < 0.001$), soluble interleukin-1 receptor-like 1 (sST2; $R = 0.29$, $p < 0.001$), cancer antigen 125 (CA-125; $R = 0.17$, $p = 0.03$), high-sensitivity C-reactive protein (hsCRP; $R = 0.20$, $p = 0.009$), and interleukin (IL)-6 ($R = 0.23$, $p = 0.003$). In contrast, IL-33 ($R = -0.01$, $p = 0.93$), IL-1 β ($R = -0.10$, $p = 0.20$), soluble neprilysin (sNEP; $R = 0.09$, $p = 0.24$), tumor necrosis factor-alpha (TNF- α ; $R = 0.07$, $p = 0.39$), and TNF- α receptor superfamily member 1A (TNFRSF1A; $R = 0.14$, $p = 0.07$) did not.

Conclusions: Total B-line sum correlated significantly, although moderately, with congestion and several inflammation biomarkers. Unexpectedly, the highest correlation found was with hsTnT.

Keywords: Biomarkers, Congestion, Diagnosis, Heart failure, Lung ultrasound, Primary care

Introduction

Heart failure (HF) diagnosis is challenging in ambulatory patients, since signs and symptoms are mild and can be related with other diseases, and even to natural aging.

Complementary tools such as lung ultrasound (LUS) and cardiac biomarkers might aid in the diagnostic approach.

LUS is highly sensitive for pulmonary congestion assessment in HF (1), since the number and distribution of B-lines denote the amount of extravascular fluid in the lung.

Current guidelines included natriuretic peptides to minimize HF diagnosis complexity, especially in the nonacute setting when echocardiography is not immediately available. In recent years, several cardiac biomarkers have been described, reflecting different active pathogenic pathways in HF (2).

The association of B-lines and N-terminal pro-brain natriuretic peptide (NT-proBNP) has been characterized in decompensated acute HF patients. Nevertheless, there are few data on outpatients, and no data with other cardiac biomarkers. Accordingly, we investigated the correlation between B-lines and different biomarkers in outpatients with suspicion of HF

Received: June 11, 2020

Accepted: September 4, 2020

Published online: October 16, 2020

Corresponding author:

Antoni Bayes-Genis
Heart Institute, Hospital Universitari Germans Trias i Pujol
Department of Medicine, Universitat Autònoma de Barcelona
Carretera del Canyet s/n 08916, Badalona - Spain
abayesgenis@gmail.com

in the primary care setting. We hypothesized that biomarkers with multiple bio-profiling other than NT-proBNP might be associated with pulmonary congestion by LUS.

Methods

Study design and patients

The present study is a biomarker subanalysis of a prospective cohort of ambulatory patients >50 years old, referred by their primary care physician to NT-proBNP test for suspected new-onset non-acute HF (July 2015 to January 2018) (3). We excluded patients with established HF diagnosis, pulmonary fibrosis, or radiological pachypleuritis. The study was performed in accordance with the Declaration of Helsinki; the local ethics committee approved the research protocol and informed consent was obtained from all subjects.

Procedures

All inclusion visits were scheduled in a centralized setting, where the primary care physician investigator (LC, MD, AW) evaluated the patients, focusing on Framingham criteria, and performed LUS. Blood samples were collected for NT-proBNP measurement (XT), and serum aliquots were stored at -80°C prior to assay (ER-L). At a subsequent visit, a cardiologist investigator (GJ) assessed all participants and performed a transthoracic Doppler echocardiogram. This physician confirmed HF diagnosis, following the European Society of Cardiology guidelines. The cardiologist had access to the patients' electronic records, including the primary care investigator visit and NT-proBNP, but was blinded to LUS and other biomarkers.

Assays

Biomarker panel

NT-proBNP, high-sensitive Troponin T (hsTnT) and growth/differentiation factor-15 (GDF-15) were measured by Cobas Elecsys[®] kits (Roche Diagnostics). Cancer antigen 125 (CA-125) was tested by ARCHITECT CA 125 II assay (Abbott Diagnostic). High-sensitivity C-reactive protein (hsCRP) was measured by hsCRP reagent (Beckman Coulter). Human soluble neprilysin (NEP) and soluble interleukin-1 receptor-like 1 (sST2) were measured by Human Soluble neprilysin/CD10 ELISA kit (Aviscera Bioscience) and Presage[®] ST2 (Critical Diagnostics) assays, respectively. Interleukin (IL)-1 β , IL-33, IL-6, tumor necrosis factor-alpha (TNF- α), and TNF- α receptor superfamily member 1A (TNFRSF1A) were tested by QuantiKine[®] immunoassay kits (R&D Systems).

NT-proBNP was analyzed after collection. The rest of the biomarkers were analyzed in the first or second freeze-thaw cycle.

Lung ultrasound

LUS was performed with a pocket device (V-scan simple model with a sectorial phased array transducer; General

Electric[®]) and interpreted bench side. LUS was performed with patient in a seated position; 8 anterolateral thoracic areas plus 4 posterior lower areas were examined. Each of the 12 areas was classified according to the number of B-lines in the sagittal scan. A thoracic area was considered positive if ≥ 3 B-lines were observed. Pleural effusion was considered as 10 B-lines. LUS congestion was defined as 2 out of 6 positive scans in each hemithorax.

Transthoracic Doppler echocardiography

Echocardiographic study was performed using an iE33 ultrasound system (Philips Medical Systems; Andover, Massachusetts) with a S5-1 sector transducer (5.1 MHz bandwidth), and analyses were performed with an EchoPAC.

Statistical analysis

Categorical values are described as absolute numbers (percentages) and continuous variables as means (standard deviations) or medians [interquartile ranges], depending on whether data distribution was normal as assessed by normal Q-Q plots. To assess the relationship of total B-line sum acquired by LUS with biomarkers' concentrations, Pearson correlation was used after logarithmic transformation of biomarker levels; afterward, partial correlations adjusted by age and sex, and finally by age, sex, body mass index, and estimated glomerular filtration rate (eGFR) were performed. Analyses were performed using Statistical Package for the Social Sciences (SPSS) 24. A two-sided $p < 0.05$ was considered significant.

Results

Table I shows baseline characteristic and biomarker values of the 170 patients included. They were elderly, predominantly women, obese or overweight, and mainly in New York Heart Association (NYHA) class II. HF diagnosis was confirmed in 38 (22.4%) patients, and only one had left ventricular ejection fraction (LVEF) $< 40\%$. Patients with HF diagnosis had higher levels of all biomarkers except IL-33, IL-1 β , and soluble neprilysin (sNEP). They also had a higher number of total B-line count ($p < 0.001$). Although 85% of patients had exertional dyspnea, only 17.1% had crackles, 9.4% orthopnea, and 3.5% paroxysmal nocturnal dyspnea.

Correlations between total B-line sum and studied biomarkers are shown in Table II. Unadjusted analyses showed that total B-line sum was significantly associated with NT-proBNP, GDF-15, hsTnT, sST2, CA-125, hsCRP, IL-6, and TNFRSF1A (R range 0.18-0.35), while IL-33, IL-1 β , sNEP, and TNF- α levels were not associated with total B-line sum. After the adjustments for the four covariates, R values tended to slightly decrease except for hsTnT and TNFRSF1A that lost statistical significance.

Discussion

Beside LUS has appeared as a step forward for HF diagnosis, and biomarkers other than NT-proBNP are currently

TABLE I - Demographic, clinical characteristics and biomarker levels of patients

| | Total n = 170 | HF diagnosis n = 38 | No HF diagnosis n = 132 | p-value |
|--------------------------------------|--------------------------|--------------------------------|------------------------------------|----------------|
| Age, years | 76 ± 10.4 | 81.2 ± 8.3 | 74.4 ± 10 | <0.001 |
| Female sex, n (%) | 115 (67.6) | 23 (60.5) | 92 (69.7) | 0.29 |
| LVEF, % | 63 ± 5.8 | 59.9 ± 7.2 | 63.8 ± 5 | <0.001 |
| Comorbidities, n (%) | | | | |
| Hypertension | 132 (77.6) | 36 (94.7) | 96 (72.7) | 0.004 |
| Diabetes mellitus | 43 (25.3) | 12 (31.6) | 31 (23.5) | 0.31 |
| COPD | 19 (11.2) | 7 (18.4) | 12 (9.1) | 0.11 |
| Valvular heart disease | 6 (3.5) | 3 (7.9) | 3 (2.3) | 0.10 |
| Myocardial infarction | 15 (8.8) | 7 (18.4) | 8 (6.1) | 0.02 |
| Atrial fibrillation | 19 (11.2) | 16 (42.1) | 3 (2.3) | <0.001 |
| Obesity (BMI >30 kg/m ²) | 84 (49.4) | 20 (52.6) | 64 (48.5) | 0.68 |
| eGFR < 60 mL/min/1.72 m ² | 48 (28.2) | 18 (47.4) | 30 (22.7) | 0.003 |
| Functional class, n (%) | | | | |
| I | 20 (11.8) | 2 (6.1) | 18 (13.6) | <0.001 |
| II | 116 (68.2) | 18 (54.5) | 98 (74.2) | |
| III | 34 (20.0) | 18 (39.4) | 16 (12.1) | |
| Exertion dyspnea | 145 (85.3) | 36 (94.7) | 109 (82.6) | 0.06 |
| Orthopnea | 16 (9.4) | 8 (21.1) | 8 (6.1) | 0.005 |
| Paroxysmal nocturnal dyspnea | 6 (3.5) | 2 (5.3) | 4 (3.0) | 0.51 |
| Lung crackles | 29 (17.1) | 11 (28.9) | 18 (13.6) | 0.03 |
| Total B-line sum | 5.6 ± 10.1 | 14.1 ± 15.0 | 3.2 ± 6.4 | <0.001 |
| Biomarkers | | | | |
| NT-proBNP, ng/L | 202 (104-640) | 1350 (666-3551) | 148 (88-289) | <0.001 |
| GDF-15, ng/L | 1708 (1175-2511) | 3133 (2040-4075) | 1470 (1113-2117) | <0.001 |
| hsTnT, ng/L | 11.9 (6.7-21.7) | 24.8 (13.8-39.9) | 9.6 (5.9-15.9) | <0.001 |
| sST2, ng/mL | 27.5 (21.8-37.6) | 39.6 (32-56.6) | 25.2 (20.7-33.8) | <0.001 |
| CA-125, U/mL | 13.7 (9.7-22.7) | 21.4 (11.4-55.4) | 13 (8.8-20) | <0.001 |
| hsCRP, mg/L | 3.4 (1.9-7.3) | 5.3 (2.3-19.2) | 3.1 (1.7-5.8) | 0.005 |
| IL-33, pg/mL | 93.7 (93.7-601.2) | 93.7 (93.7-548) | 93.7 (93.7-632.3) | 0.78 |
| IL-1β, ng/mL | 0.34 (0.27-0.44) | 0.33 (0.25-0.45) | 0.35 (0.28-0.43) | 0.60 |
| IL-6, pg/mL | 4.4 (2.9-7.2) | 6.3 (4.3-14.3) | 3.9 (2.8-5.9) | <0.001 |
| sNEP, ng/mL | 0.209 (0.062-0.605) | 0.206 (0.062-0.465) | 0.208 (0.062-0.630) | 0.62 |
| TNF-α, pg/mL | 56.3 (49.9-67.5) | 60.8 (52.7-71.1) | 55.1 (49.1-66.1) | 0.02 |
| TNFRSF1A, ng/mL | 1.88 (1.45-2.39) | 2.39 (1.72-3.56) | 1.75 (1.42-2.21) | <0.001 |

Data are expressed as mean (standard deviation), median (percentiles 25th-75th), or absolute numbers (percentages).

BMI = body mass index; CA-125 = cancer antigen 125; COPD = chronic obstructive pulmonary disease; eGFR = estimated glomerular filtration rate; GDF-15 = growth differentiation factor 15; HF = heart failure; hsCRP = high-sensitivity C-reactive protein; hsTnT = high-sensitivity troponin T; IL = interleukin; LVEF = left ventricular ejection fraction; NT-proBNP = N-terminal pro-brain natriuretic peptide; NYHA = New York Heart Association; sNEP = soluble neprilysin; sST2 = soluble interleukin-1 receptor-like 1; TNF-α = tumor necrosis factor α; TNFRSF1A = TNF receptor superfamily member 1A.

under investigation. Although there is a growing interest on both, added value for better patient diagnosis and management has scarcely been studied. In our study, we assessed the correlation between B-lines and a biomarker panel in primary care outpatients with new-onset nonacute

HF suspicion. Our results showed that (i) total B-line sum observed by LUS was significantly—although moderately—associated with several biomarkers of active pathogenic pathways in HF, especially with those related to congestion and inflammation; and (ii) hsTnT, a biomarker related to

TABLE II - Correlations between total B-line sum and studied biomarkers

| | NT-proBNP | GDF-15 | hsTnT | sST2 | CA-125 | hsCRP | IL-6 | IL-33 | IL-1 β | sNEP | TNF- α | TNFRSF1A |
|---|-----------|--------|--------|--------|--------|-------|--------|-------|--------------|------|---------------|----------|
| Unadjusted | | | | | | | | | | | | |
| R | 0.32 | 0.27 | 0.35 | 0.32 | 0.21 | 0.22 | 0.27 | -0.02 | -0.08 | 0.10 | 0.09 | 0.18 |
| p-value | <0.001 | <0.001 | <0.001 | <0.001 | 0.007 | 0.004 | <0.001 | 0.81 | 0.28 | 0.21 | 0.26 | 0.02 |
| Adjusted by age and sex | | | | | | | | | | | | |
| R | 0.29 | 0.23 | 0.34 | 0.30 | 0.19 | 0.21 | 0.24 | -0.01 | -0.11 | 0.09 | 0.08 | 0.15 |
| p-value | <0.001 | 0.003 | <0.001 | <0.001 | 0.02 | 0.007 | 0.002 | 0.93 | 0.18 | 0.24 | 0.32 | 0.06 |
| Adjusted by age, sex, BMI, and eGFR* | | | | | | | | | | | | |
| R | 0.29 | 0.23 | 0.36 | 0.29 | 0.17 | 0.20 | 0.23 | -0.01 | -0.10 | 0.09 | 0.07 | 0.14 |
| p-value | <0.001 | 0.003 | <0.001 | <0.001 | 0.03 | 0.009 | 0.003 | 0.93 | 0.20 | 0.24 | 0.39 | 0.07 |

*estimated by CKD-EPI (Chronic Kidney Disease Epidemiology Collaboration).

BMI = body mass index; CA-125 = cancer antigen 125; eGFR = estimated glomerular filtration rate; GDF-15 = growth differentiation factor 15; hsCRP = high-sensitivity C-reactive protein; hsTnT = high-sensitivity troponin T; IL = interleukin; NT-proBNP = N-terminal pro-brain natriuretic peptide; sNEP = soluble nephrilysin; sST2 = soluble interleukin-1 receptor-like 1; TNF- α = tumor necrosis factor α ; TNFRSF1A = TNF receptor superfamily member 1A.

myocardial injury, was mainly and unexpectedly associated with total B-line sum.

HF diagnosis can be difficult at early stages, especially in women and old patients with comorbidities. Our patients were elderly, mainly women, and not very symptomatic. Less than 10% of patients had lung congestion symptoms and only 17% crackles. In this context, HF was only confirmed in 22.4% of patients since Framingham criteria, despite being highly specific, have a poor sensitivity for HF diagnosis in ambulatory patients.

Hand-held devices could be easily incorporated in primary care and have shown a good correlation with standard ultrasound equipment for B-line detection. In our study, we used the 8-zone technique adding 4 posterior zones since these areas are the first that show signs of congestion and could add accuracy in outpatients.

As expected and according to previous studies in acute HF, total B-line sum was significantly associated with NT-proBNP levels. However, we projected a highest correlation, since increased intracardiac filling pressures often precede lung congestion. Nevertheless, in mildly symptomatic primary care patients, pulmonary congestion is not always present unlike hemodynamic dysfunction. sST2 levels also correlated with B-line count in a similar level that NT-proBNP. ST2 is a member of the IL-1 receptor family linked to myocardial fibrosis and adverse remodeling, both related to diastolic dysfunction and increased end-diastolic pressures that can contribute to pulmonary congestion. sST2 has been described as a 3-in-1 biomarker and provides insight into the hemodynamic, inflammatory, and pro-fibrotic/remodeling burden of the myocardium (4). Total B-line sum also correlated with GDF-15, a marker of cell injury inflammation, oxidative stress, and hypoxia. These results are consistent with previous studies where GDF-15 may indicate a greater systemic inflammatory response in old patients and those with HF and preserved EF (5), as was the population of our study. It is remarkable that these two biomarkers, being in part inflammatory biomarkers but also associated with other several

pathogenic pathways in HF, correlated with total B-line sum in a greater degree than the more "pure" inflammatory ones (hsCRP, IL-1 β , IL-33, IL-6, TNF- α , and TNFRSF1A).

Maybe the more remarkable finding was the high correlation of total B-line sum with hsTnT, a biomarker of myocardial injury frequently elevated in patients with HF without coronary ischemia. Unexpectedly, hsTnT correlation was even higher than that observed with NT-proBNP and sST2. Recently, Myhre et al (6) showed that high-sensitive cardiac Troponin T (hs-cTnT) concentrations were associated with worse diastolic function, suggesting that high levels of hs-cTnT may serve as an early marker of subclinical alterations in diastolic function that may lead to a predisposition to HF.

Finally, although there was a statistically significantly correlation between total B-line sum and CA-125, we anticipated a higher correlation, since both are surrogates of pulmonary and systemic congestion (7), respectively. Congestion plays a major role in acute HF syndromes; however, it is known that severity and organ distribution are largely heterogeneous. In fact, our primary care patients showed low percentages of congestion signs or symptoms.

Limitations of our study include the limited sample size and the low incidence of HF since our target was primary care patients with mild symptoms and suspicion of HF. These facts might have an impact on the external validity of the study. Also HF diagnosis was performed by a single cardiologist. Although larger studies in diverse populations are needed, our data are hypotheses generating correlations between B-lines, a surrogate of pulmonary congestion, and of biomarkers in HF patients.

Conclusion

In primary care outpatients with new-onset nonacute HF suspicion, total B-line sum is significantly—although moderately—associated with several biomarkers of congestion and inflammation, and remarkably with hsTnT.

Acknowledgments

The authors thank Jaume Barallat and Adriana Cserkóová for their valuable technical support in sample processing.

Disclosures

Conflict of interest: The authors declare no conflict of interest.
Financial support: This work was supported by La Marató de TV3 [PI 201510.10], the Primary Healthcare University Research Institute IDIAP-Jordi Gol, and the Catalan Society of Family Physicians (CAMFIC).

References

1. Platz E, Jhund PS, Campbell RT, McMurray JJ. Assessment and prevalence of pulmonary oedema in contemporary acute heart failure trials: a systematic review. *Eur J Heart Fail.* 2015;17:906-916.
2. Berezin AE. Prognostication in different heart failure phenotypes: the role of circulating biomarkers. *J Circ Biomark.* 2016;5:6.
3. Conangla L, Domingo M, Lupón J, et al. Lung ultrasound for heart failure diagnosis in primary care. *J Card Fail.* 2020 Jun 6:S1071-9164(19)31822-6. doi: 10.1016/j.cardfail.2020.04.019. Online ahead of print.
4. Pascual-Figal DA, Bayes-Genis A, Asensio-Lopez MC, et al. The interleukin-1 axis and risk of death in patients with acutely decompensated heart failure. *J Am Coll Cardiol.* 2019;73:1016-1025.
5. Wollert KC, Kempf T, Wallentin L. Growth differentiation factor 15 as a biomarker in cardiovascular disease. *Clin Chem.* 2017;63:140-151.
6. Myhre PL, Claggett B, Ballantyne CM, et al. Association between circulating troponin concentrations, left ventricular systolic and diastolic functions, and incident heart failure in older adults. *JAMA Cardiol.* 2019;4:997-1006.
7. Núñez J, Bayés-Genis A, Revuelta-López E, et al. Clinical role of CA125 in worsening heart failure: a BIOSTAT-CHF study subanalysis. *JACC Heart Fail.* 2020;8:386-397.

Development of an immunofluorescent AR-V7 circulating tumor cell assay – A blood-based test for men with metastatic prostate cancer

David Lu^{1,2}, Rachel Krupa¹, Melissa Harvey¹, Ryon P. Graf¹, Nicole Schreiber^{3,4}, Ethan Barnett³, Emily Carbone³, Adam Jendrisak¹, Audrey Gill¹, Sarah Orr¹, Howard I. Scher^{5,6}, Joseph D. Schonhoft¹

¹Epic Sciences, San Diego, California - USA

²Exact Sciences, Madison, Wisconsin - USA

³Department of Medicine, Memorial Sloan Kettering Cancer Center, New York, New York - USA

⁴Prostate Cancer Clinical Trials Consortium, New York, New York - USA

⁵Genitourinary Oncology Service, Department of Medicine, Memorial Sloan Kettering Cancer Center, New York, New York - USA

⁶Department of Medicine, Weill Cornell Medical College, New York, New York - USA

ABSTRACT

Introduction: Here we describe the development of a protein immunofluorescent assay for the detection of nuclear-localized androgen receptor variant 7 (AR-V7) protein within circulating tumor cells (CTCs) identified in patient blood samples. Used in the clinic, the test result serves as a validated biomarker of futility for patients with progressing metastatic castration-resistant prostate cancer (mCRPC) who are treated with androgen receptor targeted therapies (AATT) in whom nuclear-localized AR-V7 CTCs are identified and have received level 2A evidence in the 2019 National Cancer Center Network (NCCN) guidelines (v1.0).

Methods: Assay development was completed on the Epic Sciences rare cell detection platform using control cell lines of known AR-V7 status and clinical testing of mCRPC patient samples obtained at the decision point in management.

Results and conclusions: Using these samples, all assay parameters, scoring criteria, and clinical cutoffs for positivity were prospectively selected and locked. After assay lock, blinded clinical validation testing was initiated on multiple, independent, clinical cohorts as reported by Scher et al (JAMA Oncol. 2016;2:1441-1449; JAMA Oncol. 2018;4:1179-1186) and Armstrong et al (J Clin Oncol. 2019;37:1120-1129).

Keywords: AR-V7, Castration-resistant prostate cancer, Circulating tumor cells (CTCs), Predictive biomarkers

Introduction

The last decade has seen a dramatic expansion of the therapeutic options for men with recurrent metastatic castration-resistant prostate cancers (mCRPCs). In particular, next-generation androgen receptor targeted therapies (AATT) including abiraterone, enzalutamide, apalutamide, and darolutamide have unequivocally demonstrated that many CRPC

cancers remain dependent on androgen receptor signaling for growth and that these orally administered agents can improve progression-free survival and overall survival (1-7).

AATTs have quickly become the most common treatment modalities in CRPC. Abiraterone and enzalutamide received approvals in 2011 and 2012, apalutamide in 2019, and darolutamide the same year (1-7). Since then, a recent analysis of medical records of 2,559 mCRPC patients in the United States from January 2013 to September 2017 found that 1,980 (77%) received life-prolonging therapies, of whom 1,294 (65%) received an AATT as the first-line therapy. Of the 969 patients who received a second-line treatment, 523 (54%) received an AATT, with sequential use of AATTs commonly practiced (8). The second most common class of drugs utilized are taxanes, such as docetaxel or cabazitaxel (8).

While these two drug classes are the most commonly utilized in the management of mCRPC in the United States, the choice between an AATT and a taxane is often empiric without a predictive biomarker guidance (8). In this setting, the most clinically validated treatment selection biomarker

Received: June 9, 2020

Accepted: September 4, 2020

Published online: October 23, 2020

Corresponding author:

Joseph D. Schonhoft, PhD
Epic Sciences
9381 Judicial Dr.
San Diego, California 92121, USA
joseph.schonhoft@epicsciences.com

to date is the presence of nuclear-localized androgen receptor splice variant 7 (AR-V7) protein detected in the circulating tumor cells (CTCs) of metastatic CRPC patients using the Epic Sciences platform, receiving level 2A evidence in the 2019 National Cancer Center Network (NCCN) guidelines. The assay is performed at Epic Sciences as a laboratory developed test (LDT), reimbursed by the Centers for Medicare and Medicaid Services (CMS) and top private payers, has received accreditation by the College of American Pathologists (CAP), and approval from the New York State Department of Health (NYSDOH).

The first study to demonstrate clinical utility of the Epic Sciences nuclear-localized AR-V7 test was a blinded cross-sectional study consisting of mCRPC patients treated with AATT and taxanes from Memorial Sloan Kettering Cancer Center (MSKCC) (9). Both treatment-naïve (first line) and pretreated (second line or greater) patients were considered, and the results showed superior survival times for patients in whom nuclear-localized AR-V7 CTCs were identified who received a taxane compared with AATT and that favorable prostate-specific antigen (PSA) responses were observed only in the patients treated with taxanes. This study was followed by a blinded prospective validation that included mCRPC patient samples from three centers (10). Here, only second-line mCRPC-treated patients, those who had failed one prior therapy, were considered and AR-V7 biomarker-positive patients were observed to have favorable survival on taxanes compared with AATT in a risk-adjusted model, confirming our initial report. The third study, PROPHECY (NCT02269982) (11), was a prospectively designed multicenter blinded validation that included first- and second-line mCRPC patients with a poor prognosis based on a validated nomogram that included pretreatment levels of lactate dehydrogenase (LDH), alkaline phosphatase (ALK), or presence of visceral metastases among other features. All patients were treated with AATT. Here again, patients with nuclear-localized AR-V7 CTCs had a shorter time to radiographic progression, shorter overall survival, and an unfavorable PSA response (11).

Here we present the development data for the Epic Sciences nuclear-localized AR-V7 assay. Analytical and clinical feasibility testing, including control cell line screening, antibody testing, and initial patient feasibility testing, were executed to achieve assay lock prior to the commencement of the three clinical utility studies.

Materials and methods

AR-V7-positive cell line engineering

A lentiviral vector containing both EF1a-AR-V7 and RSV-puromycin inserts was transduced into a PC3 (AR-negative) parental cell line to create a stable AR-V7 expressing cell line. Target sequence integration into the cell line genome was confirmed using genomic template polymerase chain reaction (PCR). AR-V7 transfected cells were maintained under puromycin selection during culture to ensure the stable expression of AR-V7 protein. Transfected subclones were assessed via quantitative PCR (qPCR), Western blotting and immunofluorescent staining to confirm AR-V7 protein expression.

Cell culture

All cell lines were cultured using sterile techniques and complete cell culture media. To manufacture control slides for assay development and subsequent assay validation, cells were trypsinized into single-cell suspension, counted, and spiked into normal donor (ND) blood collected into Streck BCT at known quantities.

qPCR

qPCR primer pairs specific for the AR N-terminal domain (ARNTD), AR-V7 cryptic exon (ARV7CE), and the AR C-terminal domain (ARCTD) were used to assess appropriate gene expression and messenger ribonucleic acid (mRNA) splicing profiles in each cell line.

Cells were harvested and assayed for gene expression using a Single Cell-to-CT Kit (Ambion) as per manufacturer protocol. Real-time quantitative (qRT)-PCR was performed with TaqMan probes for ARNTD, ARCTD (ThermoFisher), or a probe set specific to ARV7CE (custom design) with a QuantStudio 7 (ThermoFisher). All samples were analyzed for 18S (ThermoFisher) as an internal RNA quality control.

Western blotting

Whole cell lysates were prepared using NuPAGE LDS sample buffer supplemented with 0.5% beta-mercaptoethanol and protease inhibitor. Cells were harvested via scraping from tissue culture dishes at approximately 80% confluency and sonicated via probe sonicator followed by incubation at 95°C for 5 minutes.

Protein lysates (40 µg/well) were run on NuPAGE 4%-12% Tris-Glycine precast gels and transferred using the iBlot Dry Blotting system. Overnight incubation with AR-V7 primary antibody followed by detection via WesternDot 625 goat-antirabbit kit (Cat# W10142, ThermoFisher) was used for visualization of AR-V7 protein.

All Western blotting reagents and equipment was sourced from ThermoFisher and AR-V7 antibody was sourced from Abcam (clone EP343).

Laboratory-derived sample and patient blood sample processing

Laboratory-derived (LD) control samples were created using ND blood collected into Streck cell-free blood collection tubes and spiked with either positive (GS3 or 22RV1) or negative (DU145 or PC3) cell line cells (CLCs). Contrived LD samples were used to create unequivocal positive and negative samples to mimic patient samples of known AR-V7 status. These samples were accessioned and processed identically to patient samples. For patient samples, mCRPC patient blood (7.5 mL) was collected in Streck tubes at MSKCC and processed at Epic Sciences within 48 hours. All patients gave informed consent to an institutional review board (IRB)-approved protocol before blood draw. For both LD and patient samples, red blood cells were lysed, and approximately 3 million nucleated cells were dispensed onto glass microscope slides,

fixed, and stored at -80°C as previously described (9-13). All testing presented in this study was performed prior to the start of the three clinical validation studies.

ND blood sample processing

ND blood samples were acquired from a local blood collection site (The Scripps Research Institute Normal Blood Donor Service, La Jolla, CA). Blood was drawn into Streck tubes from male donors and shipped to Epic Sciences for processing.

Immunofluorescent staining

Briefly, the immunofluorescence (IF) staining components of the assay are as follows and as previously reported (9-13). Analytical validation of the Epic Sciences platform for rare cell detection has been previously reported (12). All nucleated cells deposited onto a slide are detected with DAPI, a dye that fluoresces upon binding to deoxyribo nucleic acid (DNA) and stains the cell nucleus. White blood cells (WBCs) are detected using an anti-CD45 antibody that is directly conjugated to Alexa Fluor™ 647. CK proteins in CTCs are detected using a panel of mouse immunoglobulin G (IgG)1 anti-CK antibodies visualized with a secondary goat antimouse IgG1 antibody conjugated to Alexa Fluor™ 555. The rabbit monoclonal anti-AR-V7 antibody is recognized by a secondary goat antirabbit antibody conjugated to horseradish peroxidase (GARHRP), which catalyzes covalent binding of tyramide conjugated to Alexa Fluor™ 488.

Immunofluorescent scanning

Stained slides are scanned using the Epic Sciences automated scanning platform. The platform consists of a high-throughput microscope slide scanning system that collects images at $10\times$ magnification for each of the four fluorescent channels used in the AR-V7 assay (DAPI, CK, CD45, AR-V7). All nucleated cells found on each glass slide are imaged and mean fluorescent intensities (MFIs) are quantified. Final outputs from the fluorescent scanner include cell-level images enabling visualization of subcellular biomarker localization, MFIs for each biomarker, and unique coordinates to allow for the relocation of cells of interest for genomics or reimaging purposes.

Imaging algorithms

Using the images captured by the Epic Sciences platform, proprietary image analysis algorithms classify CTCs based on cellular morphology and biomarker MFIs detected from each of the four channels corresponding to DAPI, CK, CD45, and AR-V7. Exposure times are automatically varied to maximize signal in each field of view. For this reason, the signal quantified in a CLC or CTC subpopulation is normalized to the average signal observed in a representative population of WBCs on the slide.

The nuclear localization of AR-V7 signal (NL-ARV7) is determined based on its colocalization with DAPI (13). On a

CTC level, results are binary for the purposes of this assay. A CTC with AR-V7 fluorescent signal above background that colocalizes with DAPI is considered AR-V7 positive. Trained technical reviewers confirm the algorithm classification to identify the presence or absence of AR-V7-positive (nuclear-localized) CTCs.

Results

Control cell line characterization of AR-V7 mRNA and protein expression

To enable AR-V7 IF assay development, appropriate control cell lines (PC3, DU145, and 22RV1) were screened to confirm AR-V7 mRNA and protein expression levels. Consistent with previous reports, PC3 and DU145 cells lacked detectable AR gene expression and were negative for both AR mRNA and protein (Fig. 1A, B). 22RV1 cells are known to express several AR splice variants (14), and because of this heterogeneity, mRNA transcripts corresponding to the ARNTD-, ARV7CE-, and ARCTD-specific sequences were detected, reconfirming the expression of both full-length AR and AR-V7 splice variants (Fig. 1A).

To create an unequivocal control without the limitations of the inherent heterogeneity and lot-to-lot variability of AR variant expression in 22RV1s, we engineered a cell line to constitutively express only the AR-V7 variant. Lentiviral transfection of a PC3 parental line was used to generate several candidate subclones for constitutive AR-V7-expressing cell lines in which three were selected (GS1, GS3, GS8). While all three subclones expressed the AR-V7 transcript, only the GS3 line was found to be positive for AR-V7 protein via IF staining (Fig. 2A) and Western blot (Fig. 1B). Notably, full-length AR is not expressed in GS3 cells as evidenced by lack of detectable ARCTD transcript (Fig. 1A). For subsequent AR-V7 IF assay development, both PC3 and DU145 cells were utilized as negative controls to confirm test specificity, while 22RV1 and GS3 cells were used as positive controls.

AR-V7-specific immunofluorescent assay development

AR-V7 IF assay development utilized the Epic Sciences existing rare cell detection platform as previously described (12). Using LD samples containing either positive (GS3 or 22RV1) or negative (PC3, DU145) cells spiked into ND blood, or ND blood alone, IF staining conditions were developed and subsequently optimized (Fig. 2). Primary antibody titration results observing relative fluorescent signal in each CLC as a function of primary antibody concentration are shown in Figure 2B, C.

Upon completion of preliminary primary and secondary antibody titration curves, extensive guard banding studies were performed to confirm optimal assay parameters including primary and secondary antibody concentrations, tyramide concentration, fixation reagent concentration, fixation reagent incubation time, and wash buffer incubation times (data not shown). Final assay conditions were selected based on optimal signal-to-background ratios, yielding median

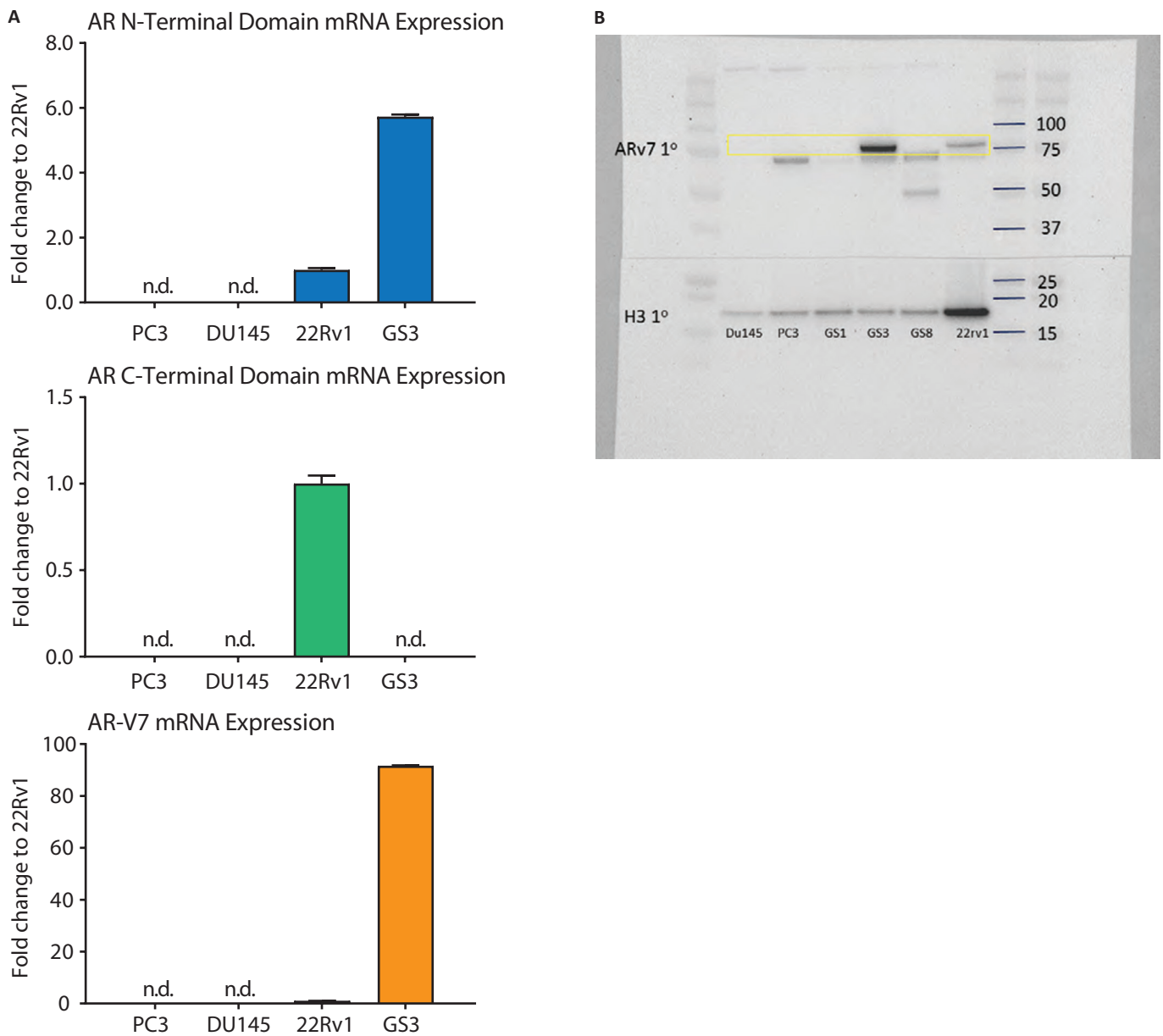


Fig. 1 - Control cell line characterization of androgen receptor variant 7 (AR-V7) messenger ribonucleic acid (mRNA) and protein expression. (A) Quantitative polymerase chain reaction analysis using AR N-terminal (ARNTD), AR C-terminal (ARCTD), and AR-V7 (ARV7CE)-specific primer sets. PC3 and DU145 cell lines are negative for all AR-specific mRNA sequences (ND: not detected). While 22RV1s expresses relatively low levels of AR-V7 transcript, ~90-fold relative abundance was observed in AR-V7 stably transfected GS3 cells. Furthermore, no ARCTD-specific transcript was observed in GS3s, confirming no full-length AR mRNA expression. mRNA abundance is quantified as fold expression compared to 22RV1. 18S is used as an internal control. (B) Western blot confirms mRNA expression profiles. DU145 and PC3 cells are AR-V7-negative, while abundant protein was observed in GS3 and 22RV1 cell lysates. GS1 and GS8 cells, alternative AR-V7 stably transfected subclones, did not produce AR-V7 protein and were discarded. Lower weight nonspecific bands (~72 kDa, 50 kDa) were observed in some cell lines. Histone H3 is used as a loading control.

AR-V7 fluorescent signals of 8.4-, 17-, and 127-fold above background in DU145, 22RV1, and GS3 cells, respectively (Fig. 2C). AR-V7 signal in positive control cells was observed to be consistently and predominantly localized in the cell nucleus, whereas signal in DU145 and PC3 was largely undetectable and if low levels were present it was non-nuclear

(example images, Fig. 2A). Therefore, hereafter, we require nuclear-specific localization of AR-V7 to call a cell positive. By comparison, similar criteria for nuclear localization have been applied to AR-V7 expression in tissue (15-17). Finally, we tested 21 ND blood donors and 0/21 (0%) were found to have AR-V7-positive CTCs.

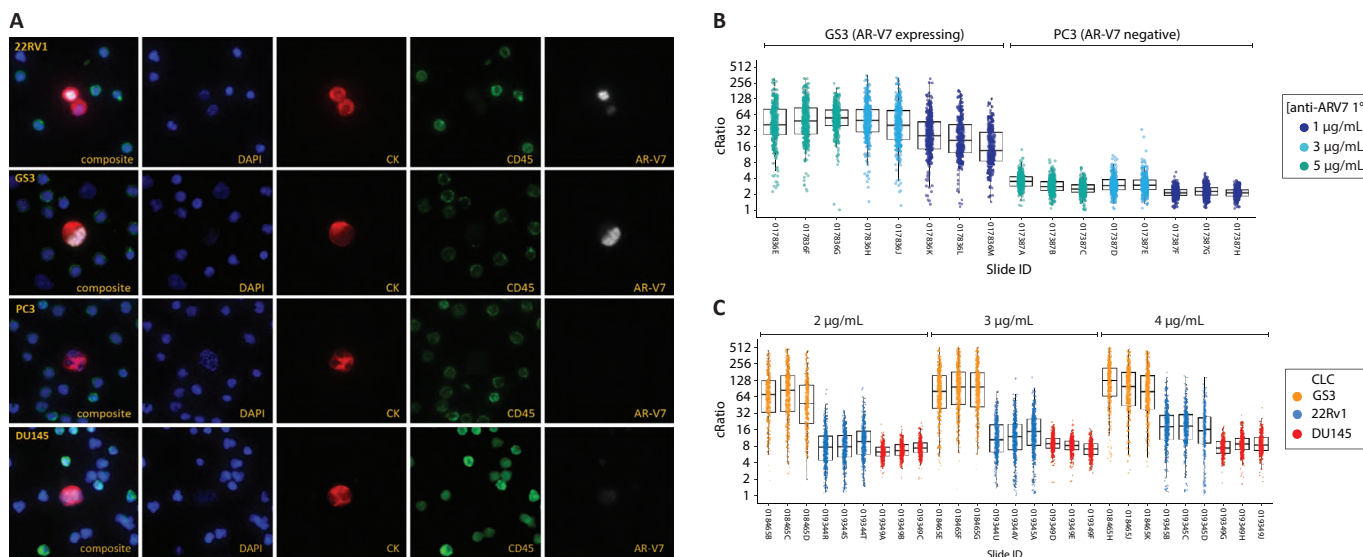


Fig. 2 - Androgen receptor variant 7 (AR-V7)-specific immunofluorescent assay development. Optimization of an immunofluorescent circulating tumor cell (CTC) assay detecting the presence of nuclear-localized AR-V7 protein was developed using control cell lines. Nuclear-localized staining was observed in 22RV1 and GS3 cells, whereas PC3 and DU145 cells are consistently negative for nuclear AR-V7 signal as seen in representative images (A). Representative microscopy images of 22RV1, GS3, PC3, DU145 cell lines. (B) Antibody titration curves comparing GS3 (AR-V7 expressing) and PC3 (AR-V7 negative). Each data point represents the mean fluorescence signal relative to the local background of a single cell detected (cRatio). (C) Titration curves comparing GS3, 22RV1, and DU145 at 2, 3, and 4 $\mu\text{g}/\text{mL}$ of AR-V7 primary antibody. At the selected primary antibody concentration of 3 $\mu\text{g}/\text{mL}$, typical fluorescent signals observed in DU145, 22RV1, and GS3 were 8.4-, 17-, and 130-fold above background, respectively. Immunofluorescent signals in negative controls (i.e., PC3, DU145) are nonzero due to a combination of cellular autofluorescence, instrument noise, and nominal nonspecific (non-nuclear) antibody binding.

Scoring criteria for AR-V7-positive cells

Before initiation of patient feasibility testing, scoring criteria were defined. For a CTC to be scored as AR-V7 positive, it must: (1) be negative for CD45 staining (blood lineage marker); (2) have CK positivity or cellular morphology indicative of epithelial (or nonhematopoietic) lineage; (3) have an intact nucleus without signs of apoptosis; and (4) have AR-V7 staining with clearly defined nuclear-localized signal. Existing clinical data indicated that AR-V7 would be more likely to be expressed in patients who had previously failed treatments in the metastatic setting (18).

To assess the general clinical feasibility of the AR-V7 assay to potentially detect physiologically relevant levels of AR-V7 protein in CTCs, 27 mCRPC patient samples were tested. These samples were obtained from patients who had previously failed at least one line of treatment in the metastatic setting, were progressing, and in need of a therapy change. Samples were not selected based on known AR-V7 status. Furthermore, this cohort was used strictly for development purposes and was not included in any subsequent clinical validation testing. Twenty-two of 27 (82%) patients harbored CTCs, 14/27 (51.8%) of patients harbored CTCs with nuclear-localized expression, and patients with AR-V7-positivity qualitatively demonstrated substantial heterogeneity, in terms of AR-V7 protein expression localization and intensity within their observed CTC populations (Fig. 3).

Based on these data, a cutoff of at least 1 AR-V7-positive CTC detected in a patient sample was prospectively chosen as

the criterion for AR-V7 test positivity. For each patient sample here, 6 million total nucleated cells were analyzed per patient sample. The detection of at least 1 positive cell was used for all subsequent clinical validation studies (9-11). Furthermore, a nuclear AR-V7 fluorescence intensity of at least 3.2-fold above background was also prospectively selected as a criterion for AR-V7 positivity based on a qualitative assessment of the mCRPC patient CTCs, that is, it was not possible to determine AR-V7 localization below this threshold. Therefore, patient samples containing CTCs with AR-V7 IF intensity below 3.2, those with non-nuclear-localized signal above 3.2, and those samples in which CTCs are not detected are classified as negative.

Discussion

In this report we present assay development results for the Epic Sciences nuclear-localized AR-V7 test. Importantly, all studies presented and all assay parameters were locked prior to initiation of any of the three clinical utility studies (9-11). The assay specifically detects the AR-V7 splice variant protein lacking the ligand binding domain in the nucleus of CTCs. Control cell line experiments demonstrate the assay's ability to distinguish between the AR-V7 truncated protein from the full-length protein and other splice variants within CTCs. Analysis of blood samples from patients with progressing mCRPC in need of a change in therapy for progressing disease were used to develop a patient scoring criteria and to demonstrate the ability of

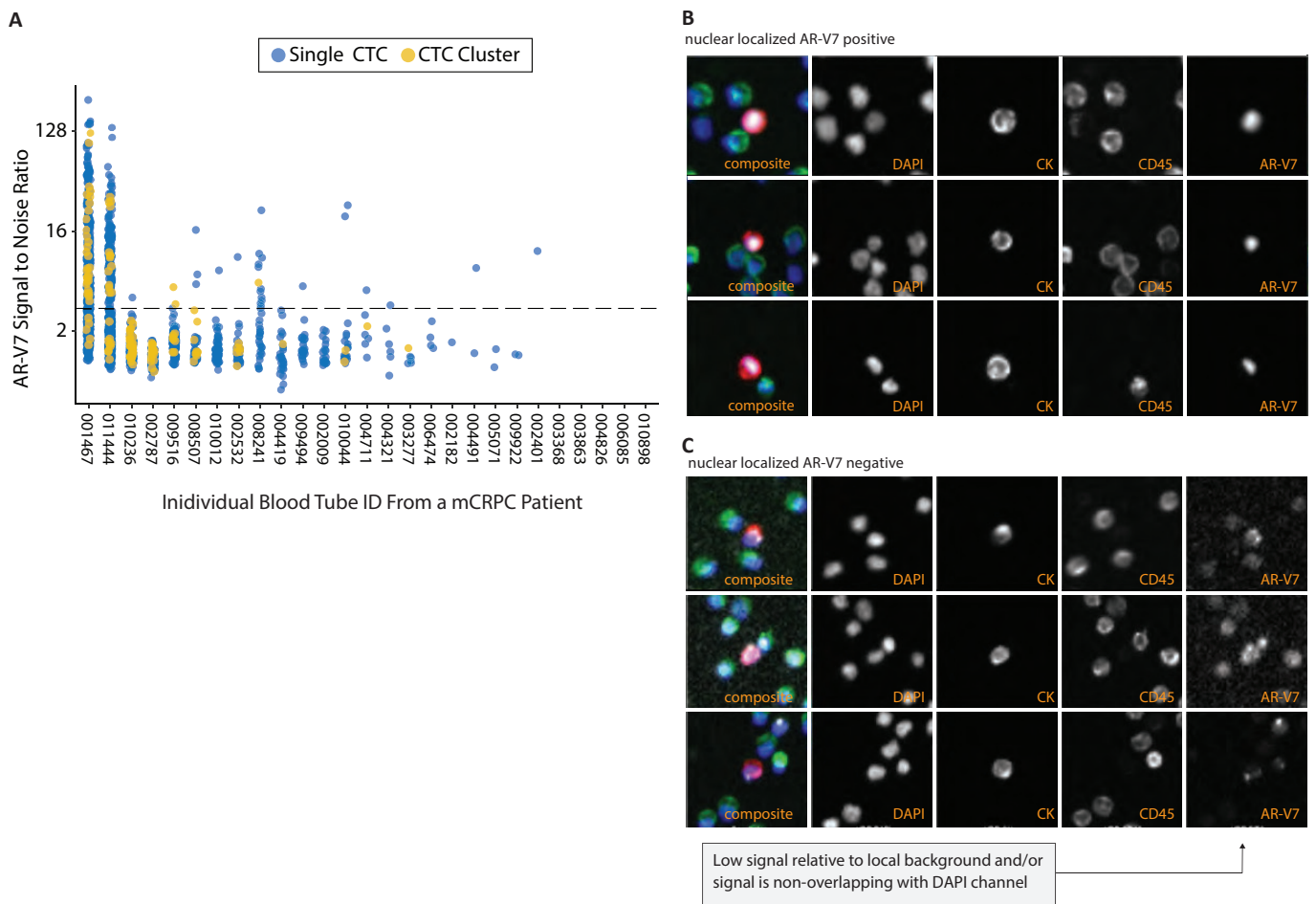


Fig. 3 - Scoring criteria for androgen receptor variant 7 (AR-V7) positive cells. Samples from 27 progressing mCRPC patients in need of a therapy change tested with the locked clinical trial assay prior to conduct of clinical utility studies. **(A)** Dot plot where every dot is one circulating tumor cell (CTC, blue) or CTC cluster (green); the y-axis indicates the immunofluorescence intensity and the x-axis indicates the unique sample identifier. Dashed line indicates the analytical cutoff for signal intensity, which combined with the presence of nuclear-localized signal constitutes a positive. Representative AR-V7-positive **(B)** and AR-V7-negative **(C)** CTC images with the following panels left to right: 4-color composite, DAPI, CK, CD45, AR-V7. Exposure times are varied to maximize signal and fluorescence intensities are reported relative to the local background.

the locked assay to specifically detect the AR-V7 protein in CTCs from patients.

The three independent clinical studies performed after assay-lock showed the clinical utility of the Epic Sciences nuclear-localized AR-V7 assay in providing information for guiding treatment selection for men with progressing mCRPCs (9-11). Specifically samples were obtained at the pertinent decision point in management and collectively show that patients in whom nuclear-localized AR-V7 protein is identified in CTCs harbor tumors that are resistant to AATs, such as abiraterone acetate or enzalutamide, and have a better chance at response and have longer survival times when treated with taxanes, such as docetaxel or cabazitaxel.

Other assays are currently available for AR-V7 detection of CTCs in the blood; however, only the nuclear-localized AR-V7 assay described here has met the Ballman criteria (19) for a predictive biomarker to date, in which two treatment groups, AATs and taxanes, have been directly

compared and a quantitative statistical interaction between biomarker, treatment group, and overall survival has been observed such as in the two studies reported by Scher et al (9,10). The most recent study, PROPHECY (11), a multicenter prospective trial, enrolled patients treated in the first and second lines with AATs and directly compared AR-V7 protein expression by the nuclear-localized AR-V7 assay with the detection of AR-V7 mRNA using qPCR from isolated CTCs' affinity enriched from blood: the Johns Hopkins AR-V7 assay (18). The nuclear-localized protein expression AR-V7 assay identified fewer AR-V7-positive patients (11% of patients having nuclear-localized AR-V7 protein vs. 24% having detectable AR-V7 mRNA in isolated CTC), although had a higher specificity of identifying nonresponse (0% vs. 11%; 50% PSA decline). While it is possible that some cells express AR-V7 mRNA, but not the functional proteins, both methods of AR-V7 detection showed a strong association with poor survival and measures of response, and

increased in frequency at progression, providing further evidence that the AR-V7 splice variant is a mechanism of AATT resistance (11).

The AR-V7 protein is a transcription factor and is required to bind to DNA in order to activate the AR signaling axis, and with this in mind, prior tissue-based assessments of AR-V7 have generally required the criteria for nuclear localization (15-17). Similarly, for CTCs it is necessary that the AR-V7 protein is nuclear localized to make a positive biomarker call and in prior clinical outcome analysis it was found that the nuclear localization is required for making treatment decisions between AATs and taxanes (13).

AATs, such as abiraterone, enzalutamide, apalutamide, and darolutamide, have been shown to extend life in CRPC (1-7); however, these treatments are not curative and nearly all patients eventually progress (20). It is hypothesized that because the AR-V7 splice variant lacks the ligand binding domain it can track into the nucleus and activate the AR signaling axis in the absence of androgens. However, other mechanisms of resistance exist, including other forms of AR reactivation, AR bypass signaling, and AR independent disease (20), and it is likely that AR-V7 expression may co-occur with many, highlighting the need for more comprehensive biomarkers that can be assessed in real time. Needed are additional blood-based CTC-based IF assays or genomic biomarkers assayed in CTCs or in circulating tumor DNA (ctDNA) to provide a more comprehensive biomarker panel to further inform therapy choice, where there are too few predictive biomarkers; the CTC nuclear-localized AR-V7 assay and tissue-based assessment of BRCA alterations for PARPi treatment are of only a few biomarkers to be reimbursed for physician choice in therapy selection to date.

Disclosures

Conflict of interest: D. Lu, R. Krupa, M. Harvey, R. Graf, J. Schonhoft, A. Jendrisak, A. Gill, S. Orr are or were employees of Epic Sciences during the writing, data collection, and analysis. H.I. Scher is a consultant/advisory board member for Ambray Genetics Corporation, Amgen, ESSA Pharma, Janssen Biotech, Janssen Research & Development, OncLive Insights, Menarini Silicon Biosystems, Physicians Education Resource, Sanofi Aventis, and WCG Oncology; and he has received institutional research funding from Epic Sciences, Illumina, Janssen Diagnostics, Menarini Silicon Biosystems, and ThermoFisher. No other disclosures are reported.

Financial support: Epic Sciences provided facilities, materials, and services to perform isolation and sequencing of circulating tumor cells. Work at Memorial Sloan Kettering Cancer Center was supported by the Sidney Kimmel Center for Prostate and Urologic Cancers, and funded in part by the NIH/NCI Cancer Center Support Grant to MSK (P30 CA008748), the NIH/NCI SPOR in Prostate Cancer grant to MSK (P50 CA092629), the Prostate Cancer Foundation, and the Prostate Cancer Clinical Trials Consortium.

References

- Beer TM, Armstrong AJ, Rathkopf DE, et al. Enzalutamide in metastatic prostate cancer before chemotherapy. *N Engl J Med.* 2014;371:424-433.
- Scher HI, Fizazi K, Saad F, et al. Increased survival with enzalutamide in prostate cancer after chemotherapy. *N Engl J Med.* 2012;367:1187-1197.
- Ryan CJ, Smith MR, Fizazi K, et al. Abiraterone acetate plus prednisone versus placebo plus prednisone in chemotherapy-naive men with metastatic castration-resistant prostate cancer (COU-AA-302): final overall survival analysis of a randomised, double-blind, placebo-controlled phase 3 study. *Lancet Oncol.* 2015;16:152-160.
- de Bono JS, Logothetis CJ, Molina A, et al. Abiraterone and increased survival in metastatic prostate cancer. *N Engl J Med.* 2011;364:1995-2005.
- Ryan CJ, Smith MR, de Bono JS, et al. Abiraterone in metastatic prostate cancer without previous chemotherapy. *N Engl J Med.* 2013;368:138-148.
- Smith MR, Saad F, Chowdhury S, et al. Apalutamide treatment and metastasis-free survival in prostate cancer. *N Engl J Med.* 2018;378:1408-1418.
- Fizazi K, Shore N, Tammela TL, et al. Darolutamide in nonmetastatic, castration-resistant prostate cancer. *N Engl J Med.* 2019;380:1235-1246.
- George DJ, Sartor O, Miller K, et al. Treatment patterns and outcomes in patients with metastatic castration-resistant prostate cancer in a real-world clinical practice setting in the United States. *Clin Genitourin Cancer.* 2020;18:284-94.
- Scher HI, Lu D, Schreiber NA, et al. Association of AR-V7 on circulating tumor cells as a treatment-specific biomarker with outcomes and survival in castration-resistant prostate cancer. *JAMA Oncol.* 2016;2:1441-1449.
- Scher HI, Graf RP, Schreiber NA, et al. Assessment of the validity of nuclear-localized androgen receptor splice variant 7 in circulating tumor cells as a predictive biomarker for castration-resistant prostate cancer. *JAMA Oncol.* 2018;4:1179-1186.
- Armstrong AJ, Halabi S, Luo J, et al. Prospective multicenter validation of androgen receptor splice variant 7 and hormone therapy resistance in high-risk castration-resistant prostate cancer: The PROPHECY Study. *J Clin Oncol.* 2019;37:1120-1129.
- Werner SL, Graf RP, Landers M, et al. Analytical validation and capabilities of the epic CTC platform: enrichment-free circulating tumour cell detection and characterization. *J Circ Biomark.* 2015;4:3.
- Scher HI, Graf RP, Schreiber NA, et al. Nuclear-specific AR-V7 protein localization is necessary to guide treatment selection in metastatic castration-resistant prostate cancer. *Eur Urol.* 2017;71:874-882.
- Hu R, Dunn TA, Wei S, et al. Ligand-independent androgen receptor variants derived from splicing of cryptic exons signify hormone-refractory prostate cancer. *Cancer Res.* 2009;69:16-22.
- Efstathiou E, Titus M, Wen S, et al. Molecular characterization of enzalutamide-treated bone metastatic castration-resistant prostate cancer. *Eur Urol.* 2015;67:53-60.
- Qu Y, Dai B, Ye D, et al. Constitutively active AR-V7 plays an essential role in the development and progression of castration-resistant prostate cancer. *Sci Rep.* 2015;5:7654.
- Welti J, Rodrigues DN, Sharp A, et al. Analytical validation and clinical qualification of a new immunohistochemical assay for androgen receptor splice variant-7 protein expression in metastatic castration-resistant prostate cancer. *Eur Urol.* 2016;70:599-608.
- Antonarakis ES, Nakazawa M, Luo J. Resistance to androgen-pathway drugs in prostate cancer. *N Engl J Med.* 2014;371:2234.
- Ballman KV. Biomarker: predictive or prognostic? *J Clin Oncol.* 2015;33:3968-3971.
- Watson PA, Arora VK, Sawyers CL. Emerging mechanisms of resistance to androgen receptor inhibitors in prostate cancer. *Nat Rev Cancer.* 2015;15:701-711.

Journal of Circulating Biomarkers

www.aboutscience.eu

ISSN 1849-4544



ABOUTSCIENCE